7

Iterative regularization methods for nonlinear problems

Finding a global minimizer of the Tikhonov function is in general not an easy task. Numerical experience shows that the Tikhonov function has usually many local minima and a descent method for solving the optimization problem may tend to get stuck especially for severely ill-posed problems. Since furthermore, the computation of an appropriate regularization parameter can require high computational effort, iterative regularization methods are an attractive alternative.

For iterative regularization methods, the number of iteration steps k plays the role of the regularization parameter, and the iterative process has to be stopped after an appropriate number of steps $k^\star$ in order to avoid an uncontrolled expansion of the noise error. In fact, a mere minimization of the residual, i.e., an ongoing iteration, leads to a semi-convergent behavior of the iterated solution: while the error in the residual decreases as the number of iteration steps increases, the error in the solution starts to increase after an initial decay. A widely used a posteriori choice for the stopping index $k^\star$ in dependence of the noise level Δ and the noisy data vector $\mathbf{y}^\delta$ is the discrepancy principle, that is, the iterative process is stopped after $k^\star$ steps such that

$$\left\|\mathbf{y}^\delta - \mathbf{F}\left(\mathbf{x}_{k^\star}^\delta\right)\right\|^2 \leq \tau\Delta^2 < \left\|\mathbf{y}^\delta - \mathbf{F}\left(\mathbf{x}_k^\delta\right)\right\|^2, \;\; 0 \leq k < k^\star, \tag{7.1}$$

with $\tau > 1$ chosen sufficiently large. In a semi-stochastic setting and for white noise with variance σ^2, the expected value of the noise $\mathcal{E}\{\|\boldsymbol{\delta}\|^2\} = m\sigma^2$ is used instead of the noise level Δ^2.

In this chapter we review the relevant iterative regularization methods and discuss practical implementation issues. We first examine an extension of the Landweber iteration to nonlinear ill-posed problems, and then address practical aspects of Newton-type methods. The application of asymptotic regularization methods to the solution of nonlinear ill-posed problems will conclude our analysis.

7.1 Nonlinear Landweber iteration

There are several ways to extend the Landweber iteration to the nonlinear case. Interpreting the Landweber iteration for the linear equation $\mathbf{K}\mathbf{x} = \mathbf{y}^\delta$ as a fixed point iteration $\mathbf{x}_{k+1} = \Phi(\mathbf{x}_k)$ with the fixed point function $\Phi(\mathbf{x}) = \mathbf{x} + \mathbf{K}^T\left(\mathbf{y}^\delta - \mathbf{K}\mathbf{x}\right)$, we replace $\mathbf{K}\mathbf{x}$ by $\mathbf{F}(\mathbf{x})$ in the expression of $\Phi(\mathbf{x})$, and obtain the so-called nonlinear Landweber iteration

$$\mathbf{x}_{k+1}^\delta = \mathbf{x}_k^\delta + \mathbf{K}_k^T \mathbf{r}_k^\delta, \quad k = 0, 1, \ldots, \tag{7.2}$$

where $\mathbf{K}_k = \mathbf{K}\left(\mathbf{x}_k^\delta\right)$ and

$$\mathbf{r}_k^\delta = \mathbf{y}^\delta - \mathbf{F}\left(\mathbf{x}_k^\delta\right). \tag{7.3}$$

Alternatively, the nonlinear Landweber iteration can be regarded as a method of steepest descent, in which the negative gradient of the nonlinear residual

$$\mathcal{F}(\mathbf{x}) = \frac{1}{2}\left\|\mathbf{y}^\delta - \mathbf{F}(\mathbf{x})\right\|^2$$

determines the update direction for the current iterate.

As in the linear case, the nonlinear Landweber iteration can only converge if the equation $\mathbf{F}(\mathbf{x}) = \mathbf{y}^\delta$ is properly scaled in the sense that

$$\|\mathbf{K}(\mathbf{x})\| \leq 1, \quad \mathbf{x} \in \mathcal{B}_\rho(\mathbf{x}_\mathtt{a}),$$

where $\mathcal{B}_\rho(\mathbf{x}_\mathtt{a})$ is a ball of radius ρ around $\mathbf{x}_\mathtt{a}$. The scaling condition can be fulfilled in practice when both sides of the nonlinear equation are multiplied by a sufficiently small constant

$$0 < \chi \leq \left[\max_{\mathbf{x} \in \mathcal{B}_\rho(\mathbf{x}_\mathtt{a})} \|\mathbf{K}(\mathbf{x})\|\right]^{-1},$$

which then in (7.2) appears as a relaxation parameter,

$$\mathbf{x}_{k+1}^\delta = \mathbf{x}_k^\delta + \chi^2 \mathbf{K}_k^T \mathbf{r}_k^\delta, \quad k = 0, 1, \ldots.$$

The nonlinear Landweber iteration (7.2) corresponds to standard-form problems with $\mathbf{L} = \mathbf{I}_n$, while for general-form problems, the iteration takes the form

$$\mathbf{x}_{k+1}^\delta = \mathbf{x}_k^\delta + \left(\mathbf{L}^T\mathbf{L}\right)^{-1} \mathbf{K}_k^T \mathbf{r}_k^\delta, \quad k = 0, 1, \ldots,$$

where $\mathbf{L}$ is a square and nonsingular regularization matrix.

This method requires a large number of iteration steps to reduce the residual norm beyond the noise level. Although several modifications of the conventional method have been proposed to ameliorate this problem (Scherzer, 1998), the computational effort remains extremely high.

7.2 Newton-type methods

For ill-posed problems, the basic concepts of the Newton method provide a reliable basis for the development of iterative regularization methods. The key idea of any Newton-type

method consists in repeatedly linearizing the nonlinear equation about some approximate solution $\mathbf{x}_k^\delta$, solving the linearized equation

$$\mathbf{K}_k \mathbf{p} = \mathbf{r}_k^\delta, \tag{7.4}$$

for the Newton step $\mathbf{p}_k^\delta$, and updating the approximate solution according to the relation

$$\mathbf{x}_{k+1}^\delta = \mathbf{x}_k^\delta + \mathbf{p}_k^\delta. \tag{7.5}$$

Equation (7.4) is typically ill-posed and to obtain a reasonable solution some sort of regularization is necessary. The type of regularization employed, or the procedure which is used to compute the Newton step, characterizes a specific iterative method.

7.2.1 Iteratively regularized Gauss–Newton method

The iteratively regularized Gauss–Newton method relies on the solution of the linearized equation

$$\mathbf{K}_k \left(\mathbf{x} - \mathbf{x}_\mathtt{a}\right) = \mathbf{y}_k^\delta, \tag{7.6}$$

with

$$\mathbf{y}_k^\delta = \mathbf{y}^\delta - \mathbf{F}\left(\mathbf{x}_k^\delta\right) + \mathbf{K}_k \left(\mathbf{x}_k^\delta - \mathbf{x}_\mathtt{a}\right),$$

by means of Tikhonov regularization with the penalty term $\left\|\mathbf{L}\left(\mathbf{x} - \mathbf{x}_\mathtt{a}\right)\right\|^2$ and the regularization parameter α_k. The new iterate minimizes the function

$$\mathcal{F}_{\mathtt{1}k}\left(\mathbf{x}\right) = \left\|\mathbf{y}_k^\delta - \mathbf{K}_k \left(\mathbf{x} - \mathbf{x}_\mathtt{a}\right)\right\|^2 + \alpha_k \left\|\mathbf{L}\left(\mathbf{x} - \mathbf{x}_\mathtt{a}\right)\right\|^2,$$

and is given by

$$\mathbf{x}_{k+1}^\delta = \mathbf{x}_\mathtt{a} + \mathbf{K}_k^\dagger \mathbf{y}_k^\delta,$$

where $\mathbf{K}_k^\dagger = \left(\mathbf{K}_k^T \mathbf{K}_k + \alpha_k \mathbf{L}^T \mathbf{L}\right)^{-1} \mathbf{K}_k^T$ is the regularized generalized inverse at the iteration step k. At first glance, this method seems to be identical to the method of Tikhonov regularization with a variable regularization parameter, but the following differences exist:

(1) the regularization parameters are the terms of a decreasing sequence satisfying the requirements

$$\alpha_k > 0, \;\; 1 < \frac{\alpha_k}{\alpha_{k+1}} \leq c, \;\; \lim_{k \to \infty} \alpha_k = 0; \tag{7.7}$$

(2) the iterative process is stopped according to the discrepancy principle (7.1) instead of requiring the convergence of iterates and employing the discrepancy principle as an a posteriori parameter choice method.

Several strategies for selecting the regularization parameters α_k can be considered. In our retrieval algorithm we use the selection criterion

$$\alpha_k = q_k \alpha_{k-1},$$

where q_k can be chosen as the ratio of a geometric sequence, i.e., $q_k = q < 1$ is constant, or as

$$q_k = \frac{\tau \Delta^2}{\left\| \mathbf{r}_k^\delta \right\|^2}, \tag{7.8}$$

and

$$q_k = 1 - \frac{\tau \Delta^2}{\left\| \mathbf{r}_k^\delta \right\|^2}. \tag{7.9}$$

With the choice (7.8) the regularization parameter decreases very fast at the beginning of iteration, while the scheme (7.9) allows enough regularization to be applied at the beginning of iteration and then to be gradually decreased.

Any iterative method using the discrepancy principle as stopping rule requires the knowledge of the noise level or of its statistical estimate $\mathcal{E}\{\|\boldsymbol{\delta}\|^2\}$. Because in many practical problems arising in atmospheric remote sensing, the errors in the data cannot be estimated (due to the forward model errors), we propose the following stopping rules:

(1) For a geometric sequence of regularization parameters, we store all iterates $\mathbf{x}_k^\delta$ and require the convergence of the nonlinear residuals $\left\| \mathbf{r}_k^\delta \right\|$ within a prescribed tolerance. If $\left\| \mathbf{r}^\delta \right\|$ is the residual at the last iteration step, we choose the solution $\mathbf{x}_{k^\star}^\delta$, with $k^\star$ being given by

$$\left\| \mathbf{r}_{k^\star}^\delta \right\|^2 \leq \tau \left\| \mathbf{r}^\delta \right\|^2 < \left\| \mathbf{r}_k^\delta \right\|^2, \ \ 0 \leq k < k^\star, \ \ \tau > 1.$$

(2) For the selection rules (7.8) and (7.9), we first estimate the noise level. For this purpose, we minimize the sum of squares

$$\mathcal{F}(\mathbf{x}) = \frac{1}{2} \left\| \mathbf{y}^\delta - \mathbf{F}(\mathbf{x}) \right\|^2$$

by requiring relative function convergence, compute the equivalent noise variance

$$\sigma_{\mathsf{e}}^2 = \frac{1}{m-n} \left\| \mathbf{r}^\delta \right\|^2,$$

where $\left\| \mathbf{r}^\delta \right\|$ is the residual at the last iteration step, and then set $\Delta^2 = m\sigma_{\mathsf{e}}^2$.

The above heuristic stopping rules do not have any mathematical justification but work sufficiently well in practice. To our knowledge there is a lack in the mathematical literature dealing with this topic and, for the time being, we do not see other viable alternatives for practical applications.

Although, from a mathematical point of view, the iteratively regularized Gauss–Newton method does not require a step-length procedure, its use may prevent the iterative process from yielding an undesirable solution. Taking into account that the Newton step $\mathbf{p}_k^\delta = \mathbf{x}_{k+1}^\delta - \mathbf{x}_k^\delta$ solves the equation

$$\mathbf{K}_{\mathtt{f}k}\left(\mathbf{x}_k^\delta\right)^T \mathbf{K}_{\mathtt{f}k}\left(\mathbf{x}_k^\delta\right) \mathbf{p} = -\mathbf{g}_k\left(\mathbf{x}_k^\delta\right),$$

where $\mathbf{g}_k$ is the gradient of the objective function

$$\mathcal{F}_k(\mathbf{x}) = \frac{1}{2}\|\mathbf{f}_k(\mathbf{x})\|^2, \quad \mathbf{f}_k(\mathbf{x}) = \begin{bmatrix} \mathbf{F}(\mathbf{x}) - \mathbf{y}^\delta \\ \sqrt{\alpha_k}\mathbf{L}(\mathbf{x} - \mathbf{x}_\mathtt{a}) \end{bmatrix},$$

and $\mathbf{K}_{\mathtt{f}k}$ is the Jacobian matrix of $\mathbf{f}_k$, we deduce that

$$\mathbf{g}_k\left(\mathbf{x}_k^\delta\right)^T \mathbf{p}_k^\delta = -\left\|\mathbf{K}_{\mathtt{f}k}\left(\mathbf{x}_k^\delta\right)\mathbf{p}_k^\delta\right\|^2 < 0,$$

and so, $\mathbf{p}_k^\delta$ is a descent direction for $\mathcal{F}_k$. Thus, the step-length procedure outlined in Algorithm 5 can be applied at each iteration step for the Tikhonov function $\mathcal{F}_k$.

In Figure 7.1 we illustrate the solution errors for the iteratively regularized Gauss–Newton method and Tikhonov regularization. In the iteratively regularized Gauss–Newton method, the exponent p characterizes the initial value of the regularization parameter, $\alpha_0 = \sigma^p$, while at all subsequent iteration steps, the regularization parameters are the terms of a geometric sequence with the ratio $q = 0.8$. The plots show that the iteratively regularized Gauss–Newton method still yields reliable results for small values of the exponent p, or equivalently, for large initial values of the regularization parameter. Evidently, a stronger regularization at the beginning of the iterative process requires a larger number of iteration steps as can be seen in the right panels of Figure 7.1. The main conclusion of this numerical simulation is that the iteratively regularized Gauss–Newton method is more stable than Tikhonov regularization with respect to overestimations of the regularization parameter.

The same results are shown in Figure 7.2 for the dynamical selection criteria (7.8) and (7.9). The selection criterion (7.8) maintains the stability of the regularization method, but the errors at small p-values are almost two times larger than those corresponding to a geometric sequence. As a result, the retrieved profiles oscillate around the exact profiles and are undersmoothed. Although the selection criterion (7.9) requires a small number of iteration steps, it is less stable with respect to overestimations of the regularization parameter. This is because we cannot find a unique value of the control parameter τ yielding accurate results over the entire domain of variation of p. For example, in the case $p = 0.3$ and the choice $\tau = 1.01$, the solution error is 0.08. Choosing $\tau = 1.05$, we reduce the solution error to 0.05, but we increase the solution error at $p = 0.5$ from 0.06 to 0.09. Thus, for the applications considered here, a dynamical selection of the regularization parameters is less reliable than an a priori selection rule using a geometric sequence (with constant ratio).

An important aspect of any iterative method using the discrepancy principle as stopping rule is the choice of the control parameter τ. From a theoretical point of view, τ should be larger than 4, but in many practical applications this choice leads to a premature termination of the iterative process. As we do not use the standard version of the discrepancy principle with known noise level, we determine the optimal value of τ by minimizing the solution error. The results plotted in Figure 7.3 show that for the O_3 and the BrO retrieval test problems, the optimal value of τ is close to 1, and we find that a good choice for τ is 1.01.

In Figure 7.4 we plot the histories of regularization parameters and residual norms for different initial values of the exponent p. The plots show that the limiting values of the sequences of regularization parameters and residual norms are comparable whatever the initial values of the regularization parameter are. These values of the regularization

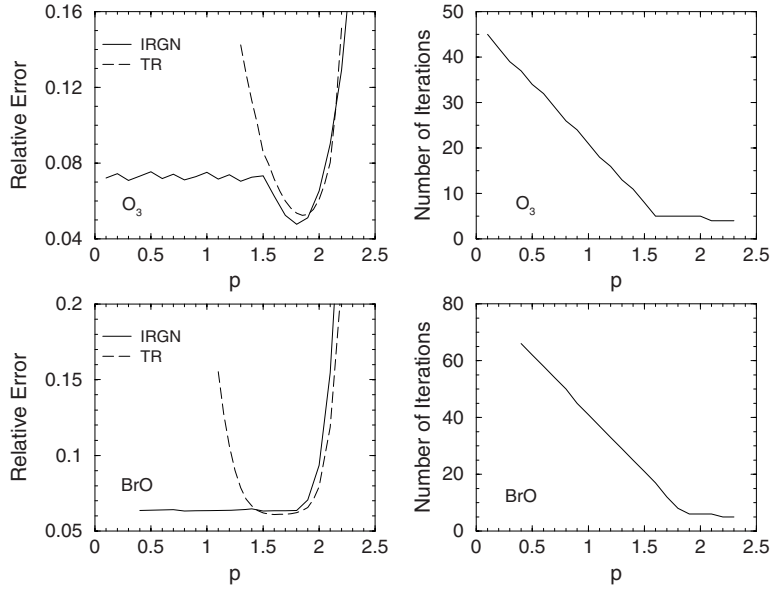

Fig. 7.1. Relative solution errors and the number of iteration steps for different values of the exponent p. The results are computed with the iteratively regularized Gauss–Newton (IRGN) method and Tikhonov regularization (TR).

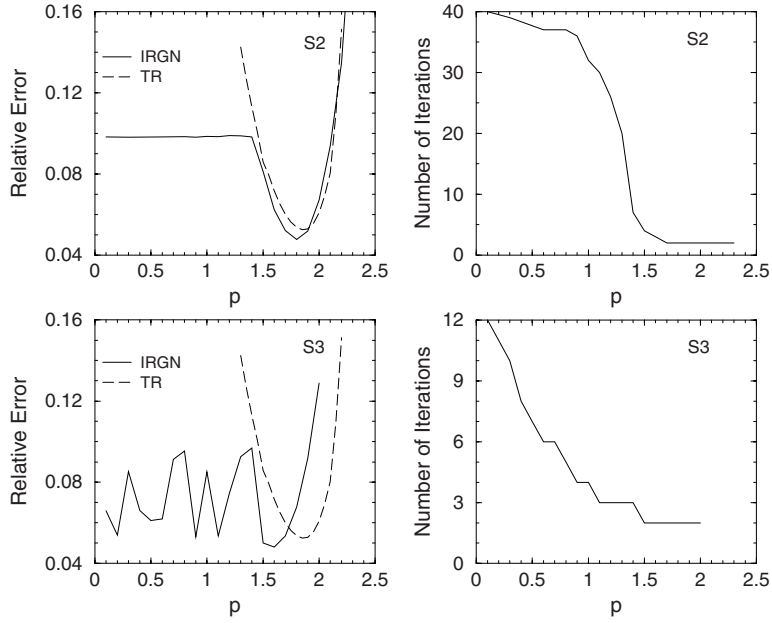

Fig. 7.2. The same as in Figure 7.1 but for the selection criteria (7.8) (S2) and (7.9) (S3). The control parameter τ is 1.01.

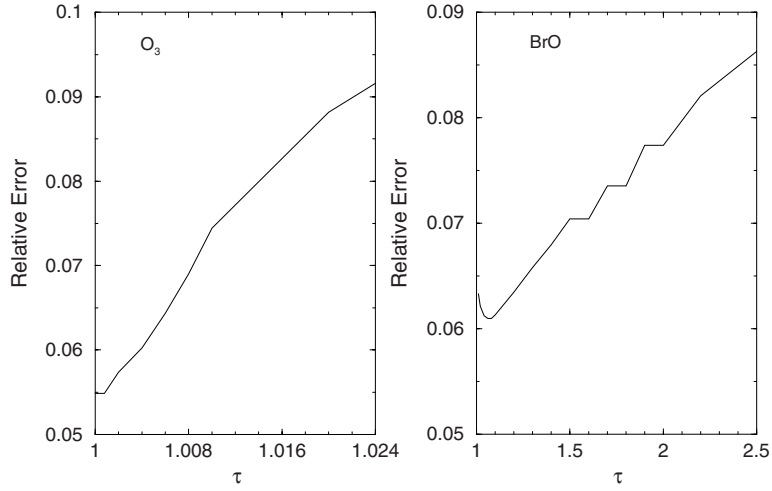

Fig. 7.3. Relative solution errors for different values of the control parameter τ.

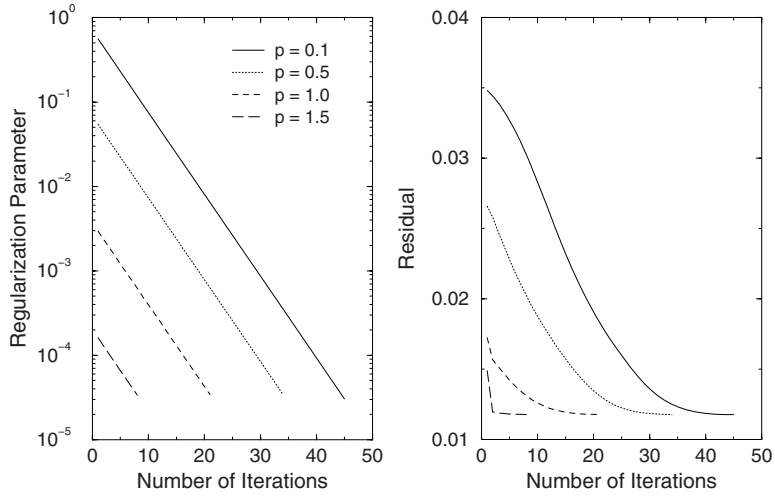

Fig. 7.4. Histories of regularization parameters and residual norms for different values of the exponent p.

parameter are $3.04 \cdot 10^{-5}$ for $p = 0.1$, $3.44 \cdot 10^{-5}$ for $p = 0.5$, $3.40 \cdot 10^{-5}$ for $p = 1.0$, and $3.37 \cdot 10^{-5}$ for $p = 1.5$. It is interesting to note that Tikhonov regularization using these limiting values as a priori regularization parameters, yields small solution errors; for the average value $\alpha = 3.31 \cdot 10^{-5}$ in Figure 7.4, the solution error for Tikhonov regularization is $5 \cdot 10^{-2}$. This equivalence suggests that we may perform an error analysis at the solution with the final value of the regularization parameter.

The retrieved profiles for the four test problems are shown in Figure 7.5. The undersmoothing effect of the selection criterion (7.8) is more pronounced for the BrO and the CO retrieval test problems.

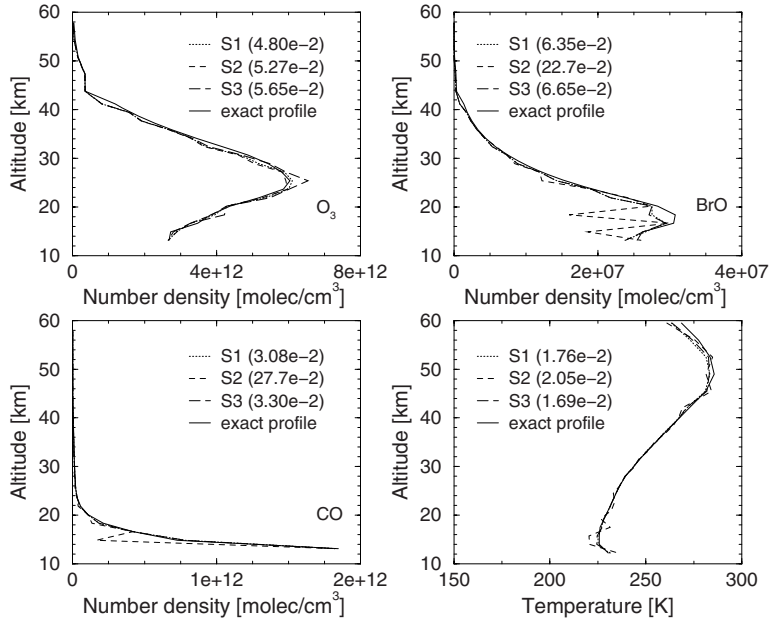

Fig. 7.5. Retrieved profiles computed with the iteratively regularized Gauss–Newton method. The results correspond to a geometric sequence of regularization parameters with a ratio of 0.8 (S1), and the selection criteria (7.8) (S2) and (7.9) (S3).

The incorporation of additional constraints into the iteratively regularized Gauss–Newton method, hereafter abbreviated as IRGN method, results in a regularization method which is less susceptible to the selection of the regularization parameter over a large range of values. For the ozone nadir sounding problem discussed in the preceding chapter, the equality-constrained IRGN method can be designed by replacing the unconstrained minimization problem

$$\min_{\triangle \mathbf{x}} \mathcal{Q}(\triangle \mathbf{x}) = \mathbf{g}^T \triangle \mathbf{x} + \frac{1}{2} \triangle \mathbf{x}^T \mathbf{G} \triangle \mathbf{x},$$

by the quadratic programming problem (cf. (6.75) and (6.76))

$$\min_{\triangle \mathbf{x}} \mathcal{Q}(\triangle \mathbf{x}) = \mathbf{g}^T \triangle \mathbf{x} + \frac{1}{2} \triangle \mathbf{x}^T \mathbf{G} \triangle \mathbf{x}$$

$$\text{subject to } \sum_{i=1}^{n} [\triangle \mathbf{x}]_i = c.$$

Here, the Hessian and the gradient of $\mathcal{Q}$ are given by $\mathbf{G} = \mathbf{K}_k^T \mathbf{K}_k + \alpha_k \mathbf{L}^T \mathbf{L}$ and $\mathbf{g} = -\mathbf{K}_k^T \mathbf{y}_k^\delta$, respectively. The quadratic programming problem is solved in the framework of the null-space method by using an explicit representation of the solution in terms of the vertical column. As opposed to the constrained Tikhonov regularization, both strengths of the constraints are now computed internally: the regularization parameter, which controls the smoothness of the solution, is decreased during the Newton iteration by a constant

factor, and the vertical column, which controls the magnitude of the solution, is determined by using the minimum distance function approach. As in general, iterative methods require more iteration steps than Tikhonov regularization, only the equality-constrained IRGN method with variable total column is appropriate for practical applications.

An inequality-constrained IRGN method can be derived if the total column is known with sufficiently accuracy. The information on the total column should be the result of an independent retrieval, which can be performed in a distinct spectral interval by using an appropriate algorithm like the DOAS approach (Van Roozendael et al., 2006; Balis et al., 2007). The proposed inequality-constrained IRGN method is of the form of the following model algorithm: at the iteration step k, compute the a priori profile deviation $\triangle\mathbf{x}^{\delta}_{k+1\alpha} = \mathbf{x}^{\delta}_{k+1\alpha} - \mathbf{x}_{\mathtt{a}}$ by solving the quadratic programming problem

$$\min_{\triangle\mathbf{x}} \mathcal{Q}\left(\triangle\mathbf{x}\right) = \mathbf{g}^T\triangle\mathbf{x} + \frac{1}{2}\triangle\mathbf{x}^T\mathbf{G}\triangle\mathbf{x} \tag{7.10}$$

$$\text{subject to } \sum_{i=1}^{n_{\mathtt{t}}} \left[\triangle\mathbf{x}\right]_i \leq c_{\max}, \tag{7.11}$$

$$\sum_{i=1}^{n} \left[\triangle\mathbf{x}\right]_i \geq c_{\min}. \tag{7.12}$$

The layer $n_{\mathtt{t}} < n$, delimits the tropospheric region from above, and the reasons for the choice (7.11)–(7.12) are the following:

(1) the constraints should be linearly independent since otherwise one of the constraints can be omitted without altering the solution;
(2) as the nadir radiance is less sensitive to variations of gas concentrations in the troposphere, the condition (7.11) does not allow large profile deviations in the sensitivity region above the troposphere;
(3) the condition (7.12) guarantees a sufficiently large deviation of the profile (with respect to the a priori) over the entire altitude range.

If c is the relative vertical column delivered by an independent retrieval and $\triangle c$ is the associated uncertainty, we may choose $c_{\min} = c - \varepsilon_{\min}\triangle c$ with $\varepsilon_{\min} \geq 1$, and $c_{\max} = c$. This choice of the upper bound is reasonable since $c_{\max}$ in (7.11) controls only the vertical column above the troposphere. The quadratic programming problem (7.10)–(7.12) can be solved by using primal and dual active set methods. The dual active set method of Goldfarb and Idnani (1983) generates dual-feasible iterates by keeping track of an active set of constraints (Appendix J). An implementation of the method of Goldfarb and Idnani is the routine 'solve.qp' from the optimization package 'quadprog', which is available free through the internet (CRAN-Package quadprog, 2007).

Considering the same retrieval scenario as in the preceding chapter and taking into account that the exact relative vertical column for ozone is $c = 110$ DU, we choose $c_{\min} = 80$ DU and $c_{\max} = 125$ DU for equality constraints, and $c_{\min} = 105$ DU and $c_{\max} = 110$ DU for inequality constraints.

In Figure 7.6 we plot the solution errors for Tikhonov regularization and the constrained and unconstrained IRGN methods. For these simulations, three values of the signal-to-noise ratio have been considered, namely 50, 100 and 150. The plots show that

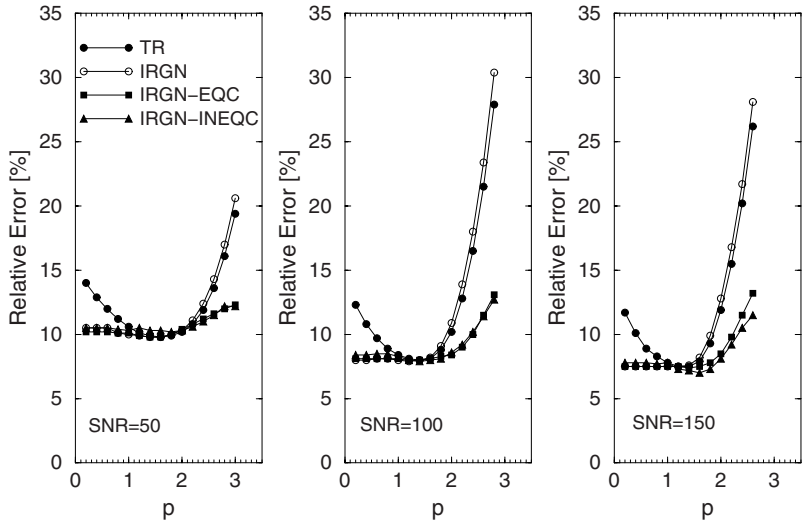

Fig. 7.6. Relative solution errors for Tikhonov regularization (TR), the IRGN method, and the equality- and inequality-constrained IRGN (IRGN-EQC and IRGN-INEQC) methods.

the constrained IRGN methods yield acceptable reconstruction errors over the entire domain of variation of the regularization parameter. The main drawback of the inequality-constrained IRGN method is its sensitivity to the selection of the bounds $c_{\min}$ and $c_{\max}$. The reason is that the method does not use an internal selection criterion for the relative vertical column and the information on c should be sufficiently accurate. Especially, the choice of the bound $c_{\min}$ is critical; we found that values smaller than 105 DU lead to large solution errors.

The retrieved profiles computed with the equality-constrained IRGN method and Tikhonov regularization are shown in Figure 7.7. For $p = 2.4$, the Tikhonov solution is undersmoothed, while for $p = 0.2$, the solution is oversmoothed in the sense that mainly the scaling and less the translation of the a priori profile is reproduced. In both situations, the profiles computed with the equality-constrained IRGN method are better approximations of the exact profile.

The computation times of the methods are outlined in Table 7.1. For $p = 0.2$, Tikhonov regularization is by a factor of 2 faster than the constrained IRGN methods, while for $p = 2.4$ their efficiencies are comparable. This enhancement of computation time is the price that we have to pay for obtaining stable approximations of the solution over a large range of values of the regularization parameter.

We conclude this section by referring to a stopping rule which can be used in conjunction with any iterative regularization method, namely the Lepskij stopping rule (Bauer and Hohage, 2005). This criterion is based on monitoring the total error

$$\mathbf{e}_k^\delta = \mathbf{e}_{\mathtt{s}k} + \mathbf{e}_{\mathtt{n}k}^\delta,$$

where the smoothing and noise errors are given by $\mathbf{e}_{\mathtt{s}k} = (\mathbf{I}_n - \mathbf{A}_{k-1})\left(\mathbf{x}^\dagger - \mathbf{x}_{\mathtt{a}}\right)$ and $\mathbf{e}_{\mathtt{n}k}^\delta = -\mathbf{K}_{k-1}^\dagger \boldsymbol{\delta}$, respectively. The idea of the Lepskij stopping rule is to use the noise

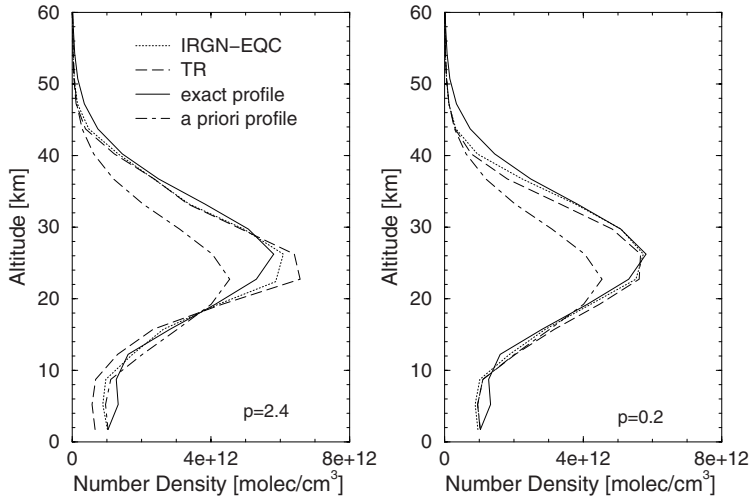

Fig. 7.7. Retrieval results corresponding to Tikhonov regularization (TR) and the equality-constrained IRGN (IRGN-EQC) method in the case SNR = 100.

Table 7.1. Computation time in min:ss format for the regularization methods in Figure 7.6. The numbers in parentheses represent the number of iteration steps and the relative solution errors expressed in percent.

	Method			
p	TR	IRGN	IRGN-EQC	IRGN-INEQC
2.4	0:20 (4;16.5)	0:23 (5;18.0)	0:26 (5;9.8)	0:24(5;9.9)
0.2	0:20 (4;12.3)	0:39 (12;8.1)	0:50 (12;8.1)	0:42(12;8.3)

error bound

$$\left\|\mathbf{e}_{\mathrm{n}k}^{\delta}\right\| \leq c_{\mathrm{n}} \frac{\Delta}{2\sqrt{\alpha_{k-1}}}, \quad c_{\mathrm{n}} \geq 1, \tag{7.13}$$

to detect the iteration step after which the total error is dominated by the noise error. By convention, the optimal stopping index $k_{\mathtt{opt}}$ is the iteration index yielding roughly a trade-off between the smoothing and noise errors. To estimate $k_{\mathtt{opt}}$, we assume that the total error can be bounded as

$$\left\|\mathbf{x}_k^{\delta} - \mathbf{x}^{\dagger}\right\| \leq \mathfrak{E}\,(k)\,\Delta, \quad k = k_{\mathtt{opt}}, \ldots, k_{\max},$$

where $\mathfrak{E} : \mathbb{N} \to [0, \infty)$ is a known increasing function. Then, using the result

$$\left\|\mathbf{x}_{k_{\mathtt{opt}}}^{\delta} - \mathbf{x}_k^{\delta}\right\| \leq \left\|\mathbf{x}_{k_{\mathtt{opt}}}^{\delta} - \mathbf{x}^{\dagger}\right\| + \left\|\mathbf{x}_k^{\delta} - \mathbf{x}^{\dagger}\right\| \leq \mathfrak{E}\left(k_{\mathtt{opt}}\right)\Delta + \mathfrak{E}\,(k)\,\Delta \leq 2\mathfrak{E}\,(k)\,\Delta$$

for all $k = k_{\mathtt{opt}} + 1, \ldots, k_{\max}$, we deduce that the optimal stopping index $k_{\mathtt{opt}}$ can be approximated by the first index $k^{\star}$ with the property

$$\left\|\mathbf{x}_{k^{\star}}^{\delta} - \mathbf{x}_k^{\delta}\right\| \leq 2\mathfrak{E}\,(k)\,\Delta, \quad k = k^{\star} + 1, \ldots, k_{\max}. \tag{7.14}$$

The stopping index $k^\star$ is called the Lepskij stopping index and (7.14) is called the Lepskij stopping rule. The main problem which has to be solved is the choice of the function $\mathfrak{E}$. Taking into account that

$$\left\|\mathbf{e}_{\mathtt{s}k_{\mathtt{opt}}}\right\| \approx \left\|\mathbf{e}^{\delta}_{\mathtt{n}k_{\mathtt{opt}}}\right\|,$$

and that

$$\left\|\mathbf{e}_{\mathtt{s}k}\right\| \leq \left\|\mathbf{e}_{\mathtt{s}k_{\mathtt{opt}}}\right\| \approx \left\|\mathbf{e}^{\delta}_{\mathtt{n}k_{\mathtt{opt}}}\right\| \leq \left\|\mathbf{e}^{\delta}_{\mathtt{n}k}\right\|, \;\; k = k_{\mathtt{opt}}, \ldots, k_{\max},$$

we obtain

$$\left\|\mathbf{x}^{\delta}_{k} - \mathbf{x}^{\dagger}\right\| \leq 2\left\|\mathbf{e}^{\delta}_{\mathtt{n}k}\right\|, \;\; k = k_{\mathtt{opt}}, \ldots, k_{\max}. \tag{7.15}$$

Thus, in a deterministic setting we may choose (cf. (7.13) and (7.15))

$$\mathfrak{E}\left(k\right) = \frac{c}{\sqrt{\alpha_{k-1}}}, \;\; c \geq 1,$$

while in a semi-stochastic setting, the estimate

$$\mathcal{E}\left\{\left\|\mathbf{e}^{\delta}_{\mathtt{n}k}\right\|^2\right\} = \sigma^2 \mathrm{trace}\left(\mathbf{K}^{\dagger}_{k-1}\mathbf{K}^{\dagger T}_{k-1}\right)$$

together with (7.15) suggests the choice

$$\mathfrak{E}\left(k\right) = c\sqrt{\frac{1}{m}\mathrm{trace}\left(\mathbf{K}^{\dagger}_{k-1}\mathbf{K}^{\dagger T}_{k-1}\right)}, \;\; c \geq 2.$$

7.2.2 Regularizing Levenberg–Marquardt method

In the regularizing Levenberg–Marquardt method, the linearized equation

$$\mathbf{K}_k\left(\mathbf{x} - \mathbf{x}^{\delta}_{k}\right) = \mathbf{r}^{\delta}_{k}, \tag{7.16}$$

with $\mathbf{r}^{\delta}_{k}$ being given by (7.3), is solved by means of Tikhonov regularization with the penalty term $\left\|\mathbf{L}\left(\mathbf{x} - \mathbf{x}^{\delta}_{k}\right)\right\|^2$ and the regularization parameter α_k. The new iterate minimizing the Tikhonov function

$$\mathcal{F}_{1k}\left(\mathbf{x}\right) = \left\|\mathbf{r}^{\delta}_{k} - \mathbf{K}_k\left(\mathbf{x} - \mathbf{x}^{\delta}_{k}\right)\right\|^2 + \alpha_k\left\|\mathbf{L}\left(\mathbf{x} - \mathbf{x}^{\delta}_{k}\right)\right\|^2, \tag{7.17}$$

is given by

$$\mathbf{x}^{\delta}_{k+1} = \mathbf{x}^{\delta}_{k} + \mathbf{K}^{\dagger}_{k}\mathbf{r}^{\delta}_{k}. \tag{7.18}$$

The difference from the iteratively regularized Gauss–Newton method consists in the penalty term which now depends on the previous iterate instead of the a priori.

The parameter choice rule $\alpha_k = q_k\alpha_{k-1}$ with $q_k < 1$, designed for the iteratively regularized Gauss–Newton method, can be used for the regularizing Levenberg–Marquardt method as well. Otherwise, the regularization parameter can be selected by applying the discrepancy principle to the linearized equation (7.16) (Hanke, 1997): if $\mathbf{p}^{\delta}_{\alpha k} = \mathbf{K}^{\dagger}_{\alpha k}\mathbf{r}^{\delta}_{k}$ with

$$\mathbf{K}^{\dagger}_{\alpha k} = \left(\mathbf{K}^{T}_{k}\mathbf{K}_k + \alpha\mathbf{L}^{T}\mathbf{L}\right)^{-1}\mathbf{K}^{T}_{k},$$

denotes the minimizer of the Tikhonov function (7.17) for an arbitrary α, the Levenberg–Marquardt parameter α_k is chosen as the solution of the 'discrepancy principle' equation

$$\left\|\mathbf{r}_k^\delta - \mathbf{K}_k \mathbf{p}_{\alpha k}^\delta\right\|^2 = \theta \left\|\mathbf{r}_k^\delta\right\|^2, \quad 0 < \theta < 1, \tag{7.19}$$

and the Newton step is taken as $\mathbf{p}_k^\delta = \mathbf{p}_{\alpha_k k}^\delta$. The regularization parameter can also be chosen according to the generalized discrepancy principle, in which case, α_k is the solution of the equation

$$\left\|\mathbf{r}_k^\delta - \mathbf{K}_k \mathbf{p}_{\alpha k}^\delta\right\|^2 - \left(\mathbf{r}_k^\delta - \mathbf{K}_k \mathbf{p}_{\alpha k}^\delta\right)^T \widehat{\mathbf{A}}_{\alpha k} \left(\mathbf{r}_k^\delta - \mathbf{K}_k \mathbf{p}_{\alpha k}^\delta\right) = \theta \left\|\mathbf{r}_k^\delta\right\|^2,$$

where $\widehat{\mathbf{A}}_{\alpha k} = \mathbf{K}_k \mathbf{K}_{\alpha k}^\dagger$ is the influence matrix.

As in the iteratively regularized Gauss–Newton method, a step-length procedure can be used to assure a decrease of the nonlinear residual at each iteration step. Considering the nonlinear residual

$$\mathcal{F}(\mathbf{x}) = \frac{1}{2} \left\|\mathbf{y}^\delta - \mathbf{F}(\mathbf{x})\right\|^2,$$

and taking into account that the gradient of $\mathcal{F}$ at $\mathbf{x}$ is given by

$$\mathbf{g}(\mathbf{x}) = -\mathbf{K}(\mathbf{x})^T \left[\mathbf{y}^\delta - \mathbf{F}(\mathbf{x})\right] = -\mathbf{K}(\mathbf{x})^T \mathbf{r}^\delta(\mathbf{x}),$$

we deduce that $\mathbf{p}_k^\delta$, solving the regularized normal equation

$$\left(\mathbf{K}_k^T \mathbf{K}_k + \alpha_k \mathbf{L}^T \mathbf{L}\right) \mathbf{p} = \mathbf{K}_k^T \mathbf{r}_k^\delta,$$

satisfies the inequality

$$\mathbf{g}\left(\mathbf{x}_k^\delta\right)^T \mathbf{p}_k^\delta = -\left(\left\|\mathbf{K}_k \mathbf{p}_k^\delta\right\|^2 + \alpha_k \left\|\mathbf{L}\mathbf{p}_k^\delta\right\|\right) < 0.$$

Thus, $\mathbf{p}_k^\delta$ is a descent direction for $\mathcal{F}$, and the objective function in Algorithm 5 is the nonlinear residual.

Instead of a step-length algorithm, a trust-region algorithm can be used to guarantee the descent condition at each iteration step. This choice is justified by the equivalence between the regularizing Levenberg–Marquardt method and a trust-region method: for a general-form regularization, the kth iteration step of the optimization problem

$$\min_{\mathbf{x}} \mathcal{F}(\mathbf{x}) = \frac{1}{2} \left\|\mathbf{y}^\delta - \mathbf{F}(\mathbf{x})\right\|^2,$$

involves the solution of the trust-region problem

$$\begin{aligned} &\min_{\mathbf{p}} \mathcal{M}_k(\mathbf{p}) \\ &\text{subject to } \|\mathbf{L}\mathbf{p}\| \le \Gamma_k, \end{aligned} \tag{7.20}$$

where

$$\mathcal{M}_k(\mathbf{p}) = \mathcal{F}\left(\mathbf{x}_k^\delta\right) - \mathbf{r}_k^{\delta T} \mathbf{K}_k \mathbf{p} + \frac{1}{2} \mathbf{p}^T \mathbf{K}_k^T \mathbf{K}_k \mathbf{p}, \tag{7.21}$$

Algorithm 11. Regularizing Levenberg–Marquardt method with a trust-region algorithm. Given the actual iterate $\mathbf{x}$ and the regularization parameter α, the algorithm computes the new iterate $\mathbf{x}_{\mathtt{new}}$ to assure a sufficient decrease of the objective function. The control parameters can be chosen as $\varepsilon_{\mathtt{f}} = 10^{-4}$, $\varepsilon_{1\Gamma} = 0.1$ and $\varepsilon_{2\Gamma} = 0.5$.

$\mathcal{F} \leftarrow 0.5 \left\| \mathbf{y}^{\delta} - \mathbf{F}(\mathbf{x}) \right\|^2$; $\quad \mathbf{g} \leftarrow -\mathbf{K}(\mathbf{x})^T \left[\mathbf{y}^{\delta} - \mathbf{F}(\mathbf{x}) \right]$;
compute the step $\mathbf{p}$ for α;
$\Gamma \leftarrow \|\mathbf{L}\mathbf{p}\|$; {trust-region radius for this step}
estimate $\Gamma_{\mathtt{min}}$; $\quad retcode \leftarrow 2$; $\quad firstcall \leftarrow$ true;
while $retcode > 1$ **do**
  if $firstcall =$ false compute the trial step $\mathbf{p}$ for the trust-region radius Γ;
  $\mathbf{x}_{\mathtt{new}} \leftarrow \mathbf{x} + \mathbf{p}$; $\quad \mathcal{F}_{\mathtt{new}} \leftarrow 0.5 \left\| \mathbf{y}^{\delta} - \mathbf{F}(\mathbf{x}_{\mathtt{new}}) \right\|^2$; $\quad \triangle\mathcal{F} \leftarrow \mathcal{F} - \mathcal{F}_{\mathtt{new}}$;
  {objective function is too large; reduce Γ and continue the while loop}
  if $\mathcal{F}_{\mathtt{new}} > \mathcal{F} + \varepsilon_{\mathtt{f}} \mathbf{g}^T \mathbf{p}$ **then**
    if $\Gamma < \Gamma_{\mathtt{min}}$ **then**
      $retcode \leftarrow 1$; $\quad \mathbf{x}_{\mathtt{new}} \leftarrow \mathbf{x}$; $\quad \mathcal{F}_{\mathtt{new}} \leftarrow \mathcal{F}$;
    else
      $retcode \leftarrow 2$; $\quad \Gamma_{\mathtt{tmp}} \leftarrow 0.5 \left(\mathbf{g}^T \mathbf{p} \right) \|\mathbf{L}\mathbf{p}\| \,/\, \left(\triangle\mathcal{F} + \mathbf{g}^T \mathbf{p} \right)$;
      if $\Gamma_{\mathtt{tmp}} < \varepsilon_{1\Gamma} \Gamma$ **then**
        $\Gamma \leftarrow \varepsilon_{1\Gamma} \Gamma$;
      else if $\Gamma_{\mathtt{tmp}} > \varepsilon_{2\Gamma} \Gamma$ **then**
        $\Gamma \leftarrow \varepsilon_{2\Gamma} \Gamma$;
      else
        $\Gamma \leftarrow \Gamma_{\mathtt{tmp}}$;
      end if
    end if
  {objective function is sufficiently small}
  else
    $retcode \leftarrow 0$;
  end if
  $firstcall \leftarrow$ false;
end while

is the quadratic Gauss–Newton model about the current iterate and Γ_k is the trust-region radius. The regularizing Levenberg–Marquardt method with a trust-region procedure is illustrated in Algorithm 11. In contrast to the standard implementation (Algorithm 6), the regularization parameter (or the Lagrange multiplier) is chosen a priori and is not determined by the trust-region radius. Only if the descent condition is violated, the trust-region radius is reduced, and the new step is computed accordingly. To compute the trial step $\mathbf{p}_k^{\delta}$ for the trust-region radius Γ_k, we consider the standard-form problem

$$\left(\bar{\mathbf{K}}_k^T \bar{\mathbf{K}}_k + \alpha \mathbf{I}_n \right) \bar{\mathbf{p}} = \bar{\mathbf{K}}_k^T \mathbf{r}_k^{\delta},$$

with $\bar{\mathbf{K}}_k = \mathbf{K}_k \mathbf{L}^{-1}$ and $\bar{\mathbf{p}} = \mathbf{L}\mathbf{p}$, solve the trust-region equation

$$\sum_{i=1}^{n} \left(\frac{\sigma_i}{\sigma_i^2 + \alpha} \right)^2 \left(\mathbf{u}_i^T \mathbf{r}_k^{\delta} \right)^2 = \Gamma_k^2, \tag{7.22}$$

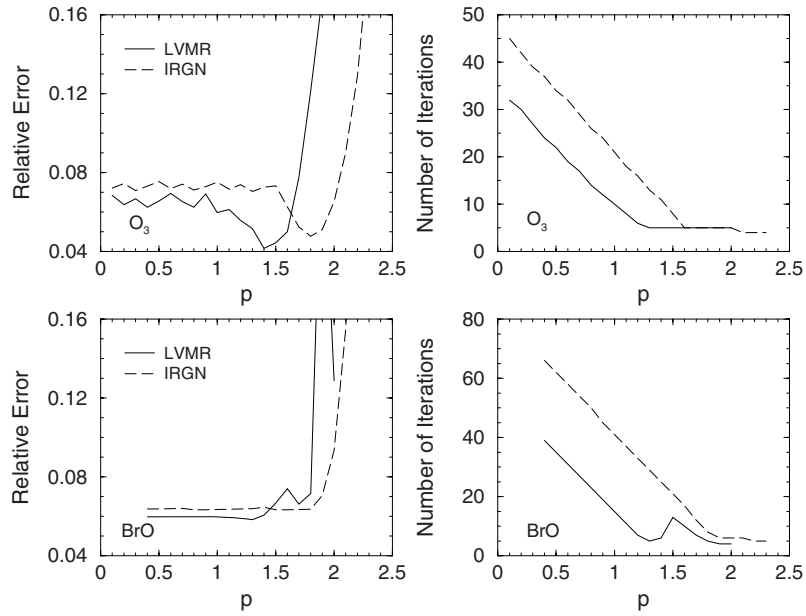

Fig. 7.8. Relative solution errors and the number of iteration steps for different values of the exponent p. The results correspond to the regularizing Levenberg–Marquardt (LVMR) method and the iteratively regularized Gauss–Newton (IRGN) method.

for $\bar{\alpha}$, where $(\sigma_i; \mathbf{v}_i, \mathbf{u}_i)$ is a singular system of $\bar{\mathbf{K}}_k$, and then set $\mathbf{p}_k^\delta = \mathbf{L}^{-1}\bar{\mathbf{p}}_{\bar{\alpha}k}^\delta$, where $\bar{\mathbf{p}}_{\bar{\alpha}k}^\delta = \bar{\mathbf{K}}_{\bar{\alpha}k}^\dagger \mathbf{r}_k^\delta$.

The regularizing Levenberg–Marquardt method is also insensitive to overestimations of the regularization parameter. The results in Figure 7.8 show that the regularizing Levenberg–Marquardt method is superior to the iteratively regularized Gauss–Newton method: for large initial values of the regularization parameter, the number of iteration steps as well as the solution errors are smaller.

The retrieved profiles illustrated in Figure 7.9 give evidence that for the BrO retrieval test problem, the undersmoothing effect of the selection criterion (7.8) is not so pronounced as in the case of the iteratively regularized Gauss–Newton method.

The results listed in Table 7.2 demonstrate that for the BrO and the CO retrieval test problems, the solution errors corresponding to the trust-region algorithm are on average smaller than those corresponding to the step-length algorithm.

The standard trust-region implementation of the Levenberg–Marquardt method (Algorithm 6) is also a regularization, in which the regularization parameter is adjusted by the trust-region radius (Wang and Yuan, 2005). However, we found that this method is very sensitive to the selection of the model parameters, especially to the choice of the amplification factor c_{a}, which controls the increase of the trust-region radius. The results in Figure 7.10 show that for large initial values of the regularization parameter we have to increase the amplification factor in order to obtain reasonable accuracies. Acceptable solutions correspond to a small domain of variations of the initial regularization parameter, and the solution errors are in general slightly larger than those corresponding to the regularizing Levenberg–Marquardt method.

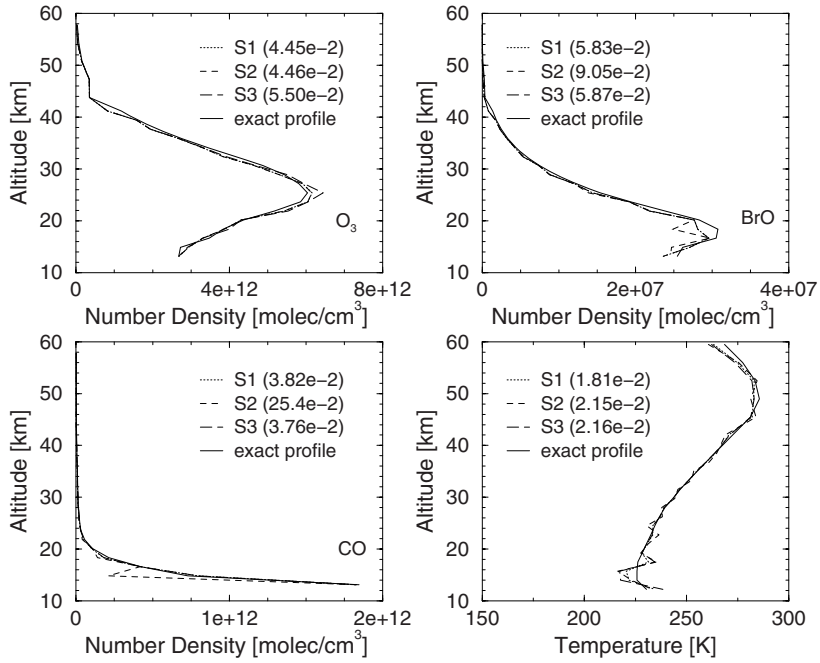

Fig. 7.9. The same as in Figure 7.5 but for the regularizing Levenberg–Marquardt method.

Table 7.2. Relative solution errors for the regularizing Levenberg–Marquardt method with the step-length and trust-region algorithms. The results correspond to a geometric sequence of regularization parameters with a ratio of 0.8 (S1), and the selection criteria (7.8) (S2) and (7.9) (S3).

		Selection criterion		
Problem	Procedure	S1	S2	S3
O_3	step-length	4.45e-2	4.46e-2	5.50e-2
	trust-region	4.41e-2	4.42e-2	5.01e-2
BrO	step-length	5.83e-2	9.05e-2	5.87e-2
	trust-region	3.54e-2	4.44e-2	3.92e-2
CO	step-length	3.82e-2	2.54e-1	3.76e-2
	trust-region	3.12e-2	1.21e-1	1.82e-2
Temperature	step-length	1.81e-2	2.16e-2	2.16e-2
	trust-region	1.96e-2	3.01e-2	2.13e-2

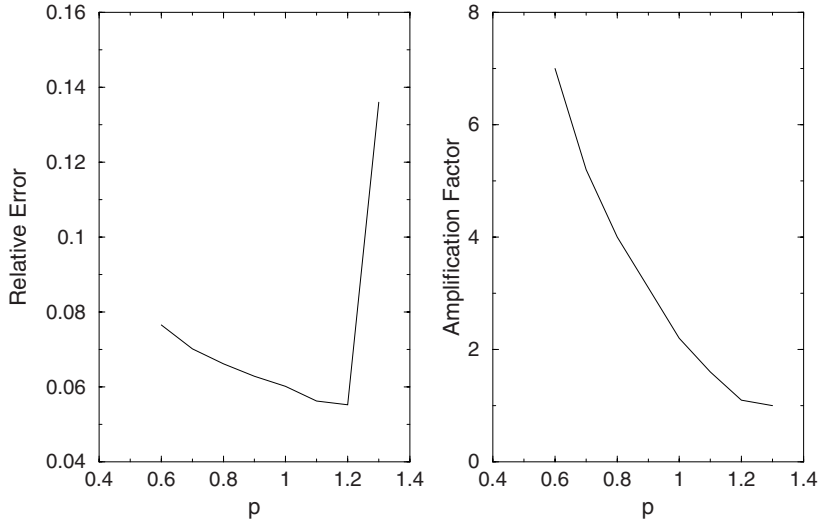

Fig. 7.10. Left: relative solution errors versus the exponent p specifying the initial value of the regularization parameter. Right: amplification factor c_{a} which controls the increase of the trust-region radius. The results correspond to the O_3 retrieval test problem.

7.2.3 Newton–CG method

The Newton–CG method relies on the solution of the linearized equation

$$\mathbf{K}_k \mathbf{p} = \mathbf{r}_k^{\delta}, \tag{7.23}$$

by means of the conjugate gradient for normal equations and by using the nonsingular regularization matrix $\mathbf{L}$ as right preconditioner. For this purpose, the CGNR or the LSQR algorithms discussed in Chapter 5 can be employed. The main peculiarity of this solution method is that the linearized equation is not solved completely; only a number of p_k iterations are performed at the Newton step k. In this regard it is apparent that the number of iteration steps p_k plays the role of the regularization parameter α_k. The resulting algorithm belongs to the class of the so-called REGINN (REGularization based on INexact Newton iteration) methods (Rieder, 1999; 2003). The term inexact Newton method refers to an approach consisting of two components:

(1) an outer Newton iteration which updates the current iterate;
(2) an inner iteration which provides the update by approximately solving a linearized version of the nonlinear equation.

It should be pointed out that other iterative methods as for example, the Landweber iteration or the ν-method, can be used for solving the linearized equation (7.23).

Algorithm 12. REGINN (REGularization based on INexact Newton iteration) algorithm. The control parameters of the algorithm are θ_0, $\theta_{\max}$, q and τ.

set $\Delta^2 = \mathcal{E}\left\{\|\boldsymbol{\delta}\|^2\right\} = m\sigma^2$ or estimate Δ^2;
$k \leftarrow 0$, $\mathbf{x}_0^\delta \leftarrow \mathbf{x_a}$;
compute $\mathbf{F}\left(\mathbf{x}_0^\delta\right)$ and $\mathbf{K}_0 = \mathbf{K}\left(\mathbf{x}_0^\delta\right)$; $\mathbf{r}_0^\delta \leftarrow \mathbf{y}^\delta - \mathbf{F}\left(\mathbf{x}_0^\delta\right)$;
$\tilde{\theta}_0 \leftarrow \theta_0$; $\tilde{\theta}_1 \leftarrow \theta_0$;
while $\left\|\mathbf{r}_k^\delta\right\|^2 > \tau\Delta^2$ **do** {discrepancy principle for the outer iteration}
  if $k > 1$ compute $\tilde{\theta}_k$ by using (7.26) ;
  $\theta_k \leftarrow \theta_{\max} \max\left(\tau\Delta^2 / \left\|\mathbf{r}_k^\delta\right\|^2, \tilde{\theta}_k\right)$;
  $l \leftarrow 0$;
  repeat
    $l \leftarrow l + 1$;
    compute $\mathbf{p}_{lk}^\delta$;
  until $\left\|\mathbf{r}_k^\delta - \mathbf{K}_k\mathbf{p}_{lk}^\delta\right\|^2 \leq \theta_k \left\|\mathbf{r}_k^\delta\right\|^2$ {discrepancy principle for the inner iteration}
  $p_k \leftarrow l$;
  $\mathbf{x}_{k+1}^\delta \leftarrow \mathbf{x}_k^\delta + \mathbf{p}_{p_k k}^\delta$;
  compute $\mathbf{F}\left(\mathbf{x}_{k+1}^\delta\right)$ and $\mathbf{K}_{k+1} = \mathbf{K}\left(\mathbf{x}_{k+1}^\delta\right)$; $\mathbf{r}_{k+1}^\delta \leftarrow \mathbf{y}^\delta - \mathbf{F}\left(\mathbf{x}_{k+1}^\delta\right)$;
  $k \leftarrow k + 1$;
end while

The REGINN method outlined in Algorithm 12 is due to Rieder (1999; 2003). The outer Newton iteration (the while loop) is stopped according to the discrepancy principle (7.1). The number of iteration steps p_k of the inner scheme (the repeat loop) is chosen according to the discrepancy principle for the linearized equation (7.23) (compare to (7.19))

$$\left\|\mathbf{r}_k^\delta - \mathbf{K}_k\mathbf{p}_{p_k k}^\delta\right\|^2 \leq \theta_k \left\|\mathbf{r}_k^\delta\right\|^2 < \left\|\mathbf{r}_k^\delta - \mathbf{K}_k\mathbf{p}_{lk}^\delta\right\|^2, \quad 1 \leq l < p_k, \tag{7.24}$$

while the following selection criterion is used for the tolerances θ_k:

(1) choose $\theta_0 \in (0,1)$ and $q \in (0,1]$;
(2) set $\tilde{\theta}_0 = \tilde{\theta}_1 = \theta_0$;
(3) compute

$$\theta_k = \theta_{\max} \max\left(\frac{\tau\Delta^2}{\left\|\mathbf{r}_k^\delta\right\|^2}, \tilde{\theta}_k\right), \tag{7.25}$$

where $\tilde{\theta}_k$ is given by

$$\tilde{\theta}_k = \begin{cases} 1 - \dfrac{p_{k-2}}{p_{k-1}}\left(1 - \theta_{k-1}\right), & p_{k-1} \geq p_{k-2}, \\ q\theta_{k-1}, & p_{k-1} < p_{k-2}, \end{cases} \quad k \geq 2, \tag{7.26}$$

and $\theta_{\max} \in (\theta_0, 1)$ bounds the θ_k away from 1 (uniformly in k and Δ).

The parameter $\theta_{\max}$ should be very close to 1, for instance, the choice $\theta_{\max} = 0.999$ is reasonable. The general idea of the selection rule (7.25)–(7.26) is to start with a small tolerance and to increase it during the Newton iteration. However, the level $\theta_k \left\|\mathbf{r}_k^\delta\right\|^2$ should

decrease during the iterative process, so that on average, the number of iteration steps p_k of the inner scheme should increase with increasing k. In the starting phase of the algorithm, the nonlinear residual is relatively large and as a result, the level $\theta_k \left\|\mathbf{r}_k^\delta\right\|^2$ is not very small even for small values of the tolerances. Thus, in spite of small tolerances, the repeat loop will terminate. From (7.26) it is apparent that the tolerance is increased when the number of passes through the repeat loop of two successive Newton steps increases significantly, and it is decreased by a constant factor whenever the consecutive numbers of passes through the repeat loop drop. However, a rapid decrease of the tolerances should be avoided (the repeat loop may not terminate) and the choice of q in the interval $[0.9, 1]$ is appropriate. In (7.25), a safeguarding technique to prevent oversolving of the discrepancy principle (especially in the final Newton step) is incorporated: at each Newton step there holds $\theta_k \left\|\mathbf{r}_k^\delta\right\|^2 \geq \tau\Delta^2$.

In our retrieval algorithm we use an a priori selection rule instead of the dynamical selection criterion (7.24): the number of iteration steps of the inner scheme is assumed to vary linearly between $p_{\min}$ and $p_{\max}$,

$$p_k = \xi^k p_{\min} + \left(1 - \xi^k\right) p_{\max}, \quad 0 < \xi < 1, \tag{7.27}$$

or according to the exponential law

$$p_k = p_{\max} - \left(p_{\max} - p_{\min}\right) \mathrm{e}^{-\xi k}. \tag{7.28}$$

In Figure 7.11 we illustrate the solution error for the selection criterion (7.27) as a function of the initial number of iteration steps of the inner scheme $p_0 = p_{\min}$. The main conclusions emerging from this simulation are summarized below.

(1) For each value of $p_{\max}$, there exists a large interval of variation of $p_{\min}$ yielding acceptable solution errors.
(2) Large values of both control parameters $p_{\min}$ and $p_{\max}$ mean large values of the number of iteration steps p_k. In this case, the regularization decreases very fast at the beginning of the iterative process, the retrieved profiles are undersmoothed and the solution errors are large.
(3) For a fixed value of $p_{\min}$, small values of $p_{\max}$ yield small values of p_k. The regularization applied at each Newton step is large, and therefore, the number of Newton steps is also large.

At each Newton step k, the number of iterations p_k of the selection criterion (7.28) is smaller than that of the selection criterion (7.27), and as a result, the number of Newton steps is larger (Figure 7.12).

7.3 Asymptotic regularization

Asymptotic regularization can be regarded as a continuous analog of the Landweber iteration,

$$\mathbf{x}_{k+1}^\delta = \mathbf{x}_k^\delta + \mathbf{K}_k^T \left[\mathbf{y}^\delta - \mathbf{F}\left(\mathbf{x}_k^\delta\right)\right], \quad k = 0, 1, \ldots.$$

In this method, a regularized approximation $\mathbf{x}^\delta(T)$ of the exact solution $\mathbf{x}^\dagger$ is obtained by solving the initial value problem (Showalter differential equation)

$$\dot{\mathbf{x}}^\delta(t) = \mathbf{K}\left(\mathbf{x}^\delta(t)\right)^T \left[\mathbf{y}^\delta - \mathbf{F}\left(\mathbf{x}^\delta(t)\right)\right], \quad 0 < t \leq T, \quad \mathbf{x}^\delta(0) = \mathbf{x}_\mathbf{a}, \tag{7.29}$$

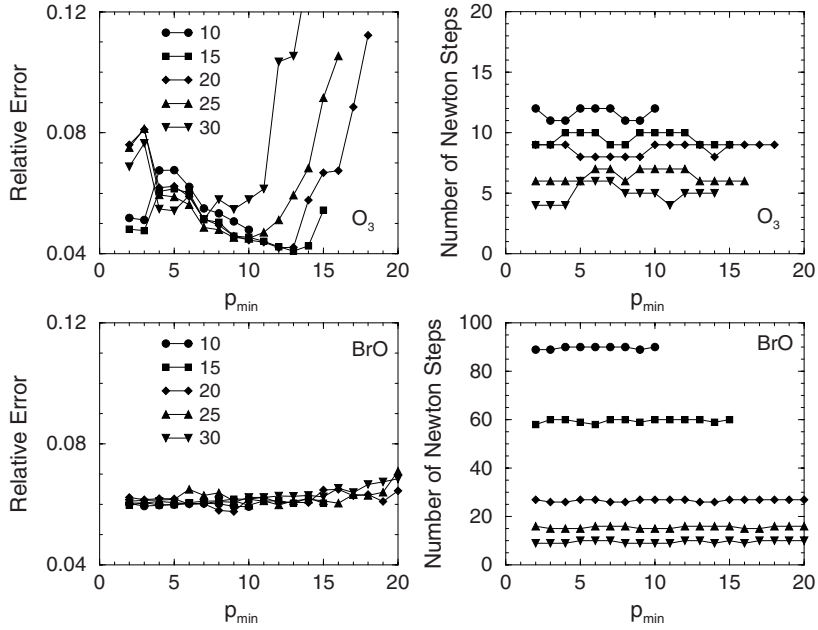

Fig. 7.11. Relative solution errors and the number of Newton steps versus $p_{\min}$ for the selection criterion (7.27) with $\xi = 0.5$. Each curve corresponds to a value of $p_{\max}$ ranging between 10 and 30.

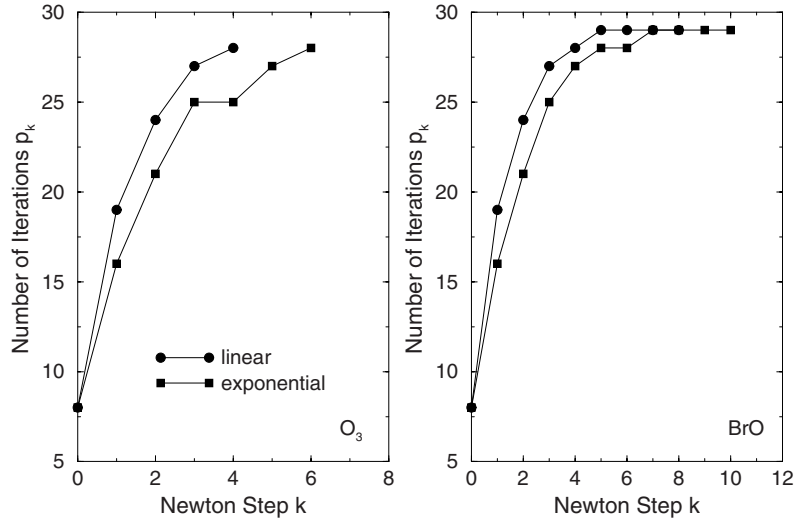

Fig. 7.12. Number of iterations p_k at each Newton step k for the linear and exponential selection rules (7.27) and (7.28), respectively.

where T plays the role of the regularization parameter. The basic property of asymptotic regularization states that $\mathbf{x}(T) \to \mathbf{x}^\dagger$ as $T \to \infty$, where $\mathbf{x}(t)$ is the solution of the noise-free problem with the exact data vector $\mathbf{y}$. For linear problems, this result is straightforward: the solution of the initial value problem

$$\dot{\mathbf{x}}(t) = \mathbf{K}^T [\mathbf{y} - \mathbf{K}\mathbf{x}(t)], \quad 0 < t \le T, \quad \mathbf{x}(0) = \mathbf{x}_\mathtt{a},$$

is given by

$$\mathbf{x}(t) = \mathrm{e}^{-\mathbf{K}^T\mathbf{K}t}\mathbf{x}_\mathtt{a} + \left(\mathbf{K}^T\mathbf{K}\right)^{-1}\left(\mathbf{I}_n - \mathrm{e}^{-\mathbf{K}^T\mathbf{K}t}\right)\mathbf{K}^T\mathbf{y},$$

whence letting $T \to \infty$, we obtain

$$\mathbf{x}(T) \to \left(\mathbf{K}^T\mathbf{K}\right)^{-1}\mathbf{K}^T\mathbf{y} = \mathbf{x}^\dagger.$$

For the nonlinear case, convergence results for the unperturbed and perturbed problems in a continuous setting have been established by Tautenhahn (1994). Applying the family of Runge–Kutta methods to the initial value problem (7.29), several iterative regularization methods have been developed by Böckmann and Pornsawad (2008). Similarly, Hochbruck et al. (2009) proposed an exponential Euler regularization method for solving the Showalter differential equation. In this section we analyze the computational efficiency of the Runge–Kutta regularization method and of the exponential Euler regularization method.

In the framework of Runge–Kutta methods, an approximate solution of the initial value problem

$$\dot{\mathbf{x}}(t) = \Psi(t, \mathbf{x}(t)), \quad \mathbf{x}(0) = \mathbf{x}_\mathtt{a},$$

is computed as

$$\begin{aligned}
\mathbf{x}_{k+1} &= \mathbf{x}_k + \tau_k \sum_{i=1}^{s} b_i \Psi(t + c_i\tau_k, \mathbf{v}_i), \\
\mathbf{v}_i &= \mathbf{x}_k + \tau_k \sum_{j=1}^{s} a_{ij} \Psi(t + c_j\tau_k, \mathbf{v}_j), \quad i = 1, \ldots, s, \quad k = 0, 1, \ldots,
\end{aligned}$$

where $\mathbf{x}_0 = \mathbf{x}_\mathtt{a}$, s is the number of stages, τ_k is the step length at the actual iteration step and the coefficients a_{ij}, b_i and c_i with $i, j = 1, \ldots, s$, depend on the particular method employed. These coefficients are usually arranged in a mnemonic device, known as the Butcher tableau (Figure 7.13).

For our purpose, we consider consistent Runge–Kutta methods with the property

$$\sum_{i=1}^{s} b_i = 1. \tag{7.30}$$

Applying the above scheme to the initial value problem (7.29) yields

$$\begin{aligned}
\mathbf{x}_{k+1}^\delta &= \mathbf{x}_k^\delta + \tau_k \sum_{i=1}^{s} b_i \mathbf{K}(\mathbf{v}_i)^T \left[\mathbf{y}^\delta - \mathbf{F}(\mathbf{v}_i)\right], \\
\mathbf{v}_i &= \mathbf{x}_k^\delta + \tau_k \sum_{j=1}^{s} a_{ij} \mathbf{K}(\mathbf{v}_j)^T \left[\mathbf{y}^\delta - \mathbf{F}(\mathbf{v}_j)\right], \quad i = 1, \ldots, s, \quad k = 0, 1, \ldots.
\end{aligned}$$

$$\begin{array}{c|ccc} c_1 & a_{11} & \dots & a_{1s} \\ \vdots & \vdots & & \vdots \\ c_s & a_{s1} & \dots & a_{ss} \\ \hline & b_1 & \dots & b_s \end{array} \qquad \begin{array}{c|c} 0 & 0 \\ \hline & 1 \end{array} \qquad \begin{array}{c|c} 1 & 1 \\ \hline & 1 \end{array}$$

(1) (2) (3)

$$\begin{array}{c|cc} 1/3 & 5/12 & -1/12 \\ 1 & 3/4 & 1/4 \\ \hline & 3/4 & 1/4 \end{array} \qquad \begin{array}{c|cc} 0 & 1/2 & -1/2 \\ 1 & 1/2 & 1/2 \\ \hline & 1/2 & 1/2 \end{array}$$

(4) (5)

Fig. 7.13. General form of a Butcher tableau (1) and specific Butcher tableaus for the explicit Euler method (2), the implicit Euler method (3), the Radau method (4), and the Lobatto method (5).

Setting

$$\mathbf{z}_i = \mathbf{v}_i - \mathbf{x}_k^\delta = \tau_k \sum_{j=1}^{s} a_{ij} \mathbf{K}\left(\mathbf{v}_j\right)^T \left[\mathbf{y}^\delta - \mathbf{F}\left(\mathbf{v}_j\right)\right],$$

and using the linearization

$$\mathbf{F}\left(\mathbf{v}_j\right) = \mathbf{F}\left(\mathbf{x}_k^\delta + \mathbf{z}_j\right) \approx \mathbf{F}\left(\mathbf{x}_k^\delta\right) + \mathbf{K}\left(\mathbf{x}_k^\delta\right) \mathbf{z}_j,$$

and the approximation

$$\mathbf{K}\left(\mathbf{v}_j\right) = \mathbf{K}\left(\mathbf{x}_k^\delta + \mathbf{z}_j\right) \approx \mathbf{K}\left(\mathbf{x}_k^\delta\right),$$

we obtain

$$\mathbf{x}_{k+1}^\delta = \mathbf{x}_k^\delta + \tau_k \sum_{i=1}^{s} b_i \mathbf{K}_k^T \left(\mathbf{r}_k^\delta - \mathbf{K}_k \mathbf{z}_i\right), \tag{7.31}$$

$$\mathbf{z}_i = \tau_k \sum_{j=1}^{s} a_{ij} \mathbf{K}_k^T \left(\mathbf{r}_k^\delta - \mathbf{K}_k \mathbf{z}_j\right), \quad i = 1, \dots, s, \quad k = 0, 1, \dots, \tag{7.32}$$

with $\mathbf{K}_k = \mathbf{K}\left(\mathbf{x}_k^\delta\right)$ and $\mathbf{r}_k^\delta = \mathbf{y}^\delta - \mathbf{F}\left(\mathbf{x}_k^\delta\right)$. To express (7.31) and (7.32) in a compact form we introduce the matrices

$$\mathsf{A} = \mathbf{A} \otimes \mathbf{I}_n, \quad \mathsf{K}_k = \mathbf{I}_s \otimes \mathbf{K}_k, \quad \mathsf{B} = \mathbf{b}^T \otimes \mathbf{I}_n, \quad \mathsf{I} = \mathbf{I}_s \otimes \mathbf{I}_n,$$

and the vectors

$$\mathsf{r}_k^\delta = \mathbf{1}_s \otimes \mathbf{r}_k^\delta, \quad \mathsf{z} = \begin{bmatrix} \mathbf{z}_1 \\ \vdots \\ \mathbf{z}_s \end{bmatrix} \in \mathbb{R}^{sn},$$

where

$$\mathbf{A} = \begin{bmatrix} a_{11} & \dots & a_{1s} \\ \vdots & \ddots & \vdots \\ a_{s1} & \dots & a_{ss} \end{bmatrix} \in \mathbb{R}^{s \times s}, \quad \mathbf{b} = \begin{bmatrix} b_1 \\ \vdots \\ b_s \end{bmatrix} \in \mathbb{R}^s, \quad \mathbf{1}_s = \begin{bmatrix} 1 \\ \vdots \\ 1 \end{bmatrix} \in \mathbb{R}^s,$$

and the notation $\mathbf{X} \otimes \mathbf{Y}$ stands for the Kronecker product of the matrices $\mathbf{X} \in \mathbb{R}^{m\times n}$ and $\mathbf{Y} \in \mathbb{R}^{p\times q}$ defined as

$$\mathbf{X} \otimes \mathbf{Y} = \begin{bmatrix} x_{11}\mathbf{Y} & \dots & x_{1n}\mathbf{Y} \\ \vdots & \ddots & \vdots \\ x_{m1}\mathbf{Y} & \dots & x_{mn}\mathbf{Y} \end{bmatrix} \in \mathbb{R}^{mp\times nq}, \;\; [\mathbf{X}]_{ij} = x_{ij}.$$

The use of the Kronecker product enables us to derive a transparent solution representation in a straightforward manner. When working with the Kronecker product, the following calculation rules have to be taken into account: for compatible matrices $\mathbf{X}$, $\mathbf{Y}$, $\mathbf{Z}$ and $\mathbf{W}$, there hold

$$(\mathbf{X} \otimes \mathbf{Y})\,(\mathbf{Z} \otimes \mathbf{W}) = \mathbf{XZ} \otimes \mathbf{YW}, \tag{7.33}$$

$$(\mathbf{X} \otimes \mathbf{Y})^T = \mathbf{X}^T \otimes \mathbf{Y}^T, \tag{7.34}$$

$$(\mathbf{X} \otimes \mathbf{Y})^{-1} = \mathbf{X}^{-1} \otimes \mathbf{Y}^{-1}. \tag{7.35}$$

Moreover, if $\mathsf{A} = \mathbf{A} \otimes \mathbf{I}_n$ with $\mathbf{A} \in \mathbb{R}^{s\times s}$ and $\mathsf{X} = \mathbf{I}_s \otimes \mathbf{X}$ with $\mathbf{X} \in \mathbb{R}^{n\times n}$, then the representations

$$\mathsf{AX} = (\mathbf{A} \otimes \mathbf{I}_n)\,(\mathbf{I}_s \otimes \mathbf{X}) = \mathbf{A} \otimes \mathbf{X}$$

and

$$\mathsf{XA} = (\mathbf{I}_s \otimes \mathbf{X})\,(\mathbf{A} \otimes \mathbf{I}_n) = \mathbf{A} \otimes \mathbf{X},$$

yield the symmetry relation

$$\mathsf{AX} = \mathsf{XA}. \tag{7.36}$$

Now, using the consistency relation (7.30), (7.31) and (7.32) become

$$\mathbf{x}_{k+1}^{\delta} = \mathbf{x}_k^{\delta} + \tau_k \mathbf{K}_k^T \mathbf{r}_k^{\delta} - \tau_k \mathsf{B}\mathsf{K}_k^T \mathsf{K}_k \mathsf{z}, \tag{7.37}$$

$$\left(\tau_k \mathsf{A}\mathsf{K}_k^T \mathsf{K}_k + \mathsf{I}\right) \mathsf{z} = \tau_k \mathsf{A}\mathsf{K}_k^T \mathsf{r}_k^{\delta}. \tag{7.38}$$

Equation (7.38) is solved for z,

$$\mathsf{z} = \tau_k \left(\tau_k \mathsf{A}\mathsf{K}_k^T \mathsf{K}_k + \mathsf{I}\right)^{-1} \mathsf{A}\mathsf{K}_k^T \mathsf{r}_k^{\delta},$$

and is rearranged in the form

$$\mathsf{B}\mathsf{K}_k^T \mathsf{K}_k \mathsf{z} = \mathsf{B}\mathsf{K}_k^T \mathsf{r}_k^{\delta} - \mathsf{B}\mathsf{A}^{-1} \left(\tau_k \mathsf{A}\mathsf{K}_k^T \mathsf{K}_k + \mathsf{I}\right)^{-1} \mathsf{A}\mathsf{K}_k^T \mathsf{r}_k^{\delta}. \tag{7.39}$$

Since $\mathbf{b}^T \mathbf{1}_s = 1$ and $\mathbf{X} = 1 \otimes \mathbf{X}$, we have

$$\mathsf{B}\mathsf{K}_k^T \mathsf{r}_k^{\delta} = \left(\mathbf{b}^T \otimes \mathbf{I}_n\right) \left(\mathbf{I}_s \otimes \mathbf{K}_k^T\right) \left(\mathbf{1}_s \otimes \mathbf{r}_k^{\delta}\right) = \mathbf{K}_k^T \mathbf{r}_k^{\delta}, \tag{7.40}$$

and by virtue of (7.39) and (7.40), (7.37) can be written as

$$\mathbf{x}_{k+1}^{\delta} = \mathbf{x}_k^{\delta} + \tau_k \mathsf{B}\mathsf{A}^{-1} \left(\tau_k \mathsf{A}\mathsf{K}_k^T \mathsf{K}_k + \mathsf{I}\right)^{-1} \mathsf{A}\mathsf{K}_k^T \mathsf{r}_k^{\delta}.$$

Finally, introducing the regularization parameter α_k by

$$\alpha_k = \frac{1}{\tau_k},$$

and using the symmetry relation (cf. (7.36) and the identity $\mathsf{K}_k^T\mathsf{K}_k = \mathbf{I}_s \otimes \mathbf{K}_k^T\mathbf{K}_k$)

$$\mathsf{A}\left(\mathsf{K}_k^T\mathsf{K}_k\right) = \left(\mathsf{K}_k^T\mathsf{K}_k\right)\mathsf{A},$$

which yields,

$$\mathsf{A}^{-1}\left(\mathsf{A}\mathsf{K}_k^T\mathsf{K}_k + \alpha_k\mathsf{I}\right)^{-1}\mathsf{A} = \left(\mathsf{A}\mathsf{K}_k^T\mathsf{K}_k + \alpha_k\mathsf{I}\right)^{-1},$$

we obtain the iteration of the Runge–Kutta regularization method

$$\mathbf{x}_{k+1}^\delta = \mathbf{x}_k^\delta + \mathsf{B}\left(\mathsf{A}\mathsf{K}_k^T\mathsf{K}_k + \alpha_k\mathsf{I}\right)^{-1}\mathsf{K}_k^T\mathsf{r}_k^\delta, \quad k = 0, 1, \ldots. \tag{7.41}$$

It is remarkable to note that for the explicit Euler iteration ($s = 1$, $a_{11} = 0$, $b_1 = 1$) we are led to $\mathbf{z}_1 = \mathbf{0}$, and (7.31) is the iteration of the nonlinear Landweber method (with a relaxation parameter τ_k). Furthermore, for the implicit Euler method ($s = 1$, $a_{11} = 1$, $b_1 = 1$) there holds

$$\mathsf{A} = \mathsf{B} = \mathbf{I}_n, \quad \mathsf{K}_k = \mathbf{K}_k, \quad \mathsf{r}_k^\delta = \mathbf{r}_k^\delta,$$

and (7.41) is the iteration of the regularizing Levenberg–Marquardt method with $\mathbf{L} = \mathbf{I}_n$, i.e.,

$$\mathbf{x}_{k+1}^\delta = \mathbf{x}_k^\delta + \left(\mathbf{K}_k^T\mathbf{K}_k + \alpha_k\mathbf{I}_n\right)^{-1}\mathbf{K}_k^T\mathbf{r}_k^\delta, \quad k = 0, 1, \ldots. \tag{7.42}$$

The regularizing property of any inversion method discussed up to now is reflected by the filter factors. This concept can be generalized by introducing the so-called filter matrix. For example, if $(\sigma_i; \mathbf{v}_i, \mathbf{u}_i)$ is a singular system of the matrix $\mathbf{K}_k$, then the iterate of the regularizing Levenberg–Marquardt method (7.42) can be expressed as

$$\mathbf{x}_{k+1}^\delta = \mathbf{x}_k^\delta + \mathbf{V}\mathbf{F}_k \begin{bmatrix} \frac{1}{\sigma_1}\mathbf{u}_1^T\mathbf{r}_k^\delta \\ \vdots \\ \frac{1}{\sigma_n}\mathbf{u}_n^T\mathbf{r}_k^\delta \end{bmatrix}, \tag{7.43}$$

where the diagonal matrix

$$\mathbf{F}_k = \left[\operatorname{diag}\left(f_{\alpha_k}\left(\sigma_i^2\right)\right)_{n\times n}\right], \quad f_k\left(\sigma_i^2\right) = \frac{\sigma_i^2}{\sigma_i^2 + \alpha_k}, \tag{7.44}$$

represents the filter matrix. Evidently, for very small values of the regularization parameter, $\mathbf{F}_k \approx \mathbf{I}_n$, while for very large values of the regularization parameter $\mathbf{F}_k \approx (1/\alpha_k)\left[\operatorname{diag}\left(\sigma_i^2\right)_{n\times n}\right]$. For the Runge–Kutta regularization method, the filter matrix is not diagonal because A is not diagonal. To derive the expression of the filter matrix in this case, we first employ the relations (cf. (7.33))

$$\mathsf{A}\mathsf{K}_k^T\mathsf{K}_k = \mathbf{A} \otimes \left(\mathbf{K}_k^T\mathbf{K}_k\right) = \left(\mathbf{I}_s \otimes \mathbf{V}\right)\left(\mathbf{A} \otimes \left[\operatorname{diag}\left(\sigma_i^2\right)_{n\times n}\right]\right)\left(\mathbf{I}_s \otimes \mathbf{V}^T\right)$$

and

$$\alpha_k\mathsf{I} = \left(\mathbf{I}_s \otimes \mathbf{V}\right)\left(\alpha_k\mathsf{I}\right)\left(\mathbf{I}_s \otimes \mathbf{V}^T\right)$$

to obtain

$$\mathsf{A}\mathsf{K}_k^T\mathsf{K}_k + \alpha_k\mathsf{I} = \left(\mathbf{I}_s \otimes \mathbf{V}\right)\left(\mathbf{A} \otimes \left[\operatorname{diag}\left(\sigma_i^2\right)_{n\times n}\right] + \alpha_k\mathsf{I}\right)\left(\mathbf{I}_s \otimes \mathbf{V}^T\right).$$

Then, we use

$$\mathsf{K}_k^T \mathsf{r}_k^\delta = \mathbf{1}_s \otimes \left(\mathbf{K}_k^T \mathbf{r}_k^\delta\right) = \left(\mathbf{I}_s \otimes \mathbf{V}\right) \left(\mathbf{I}_s \otimes \left[\operatorname{diag}\left(\sigma_i^2\right)_{n\times n}\right]\right) \left(\mathbf{1}_s \otimes \begin{bmatrix} \frac{1}{\sigma_1}\mathbf{u}_1^T \mathbf{r}_k^\delta \\ \vdots \\ \frac{1}{\sigma_n}\mathbf{u}_n^T \mathbf{r}_k^\delta \end{bmatrix}\right),$$

and

$$\mathsf{B}\left(\mathbf{I}_s \otimes \mathbf{V}\right) = \left(\mathbf{b}^T \otimes \mathbf{I}_n\right)\left(\mathbf{I}_s \otimes \mathbf{V}\right) = \mathbf{b}^T \otimes \mathbf{V},$$

together with (cf. (7.35))

$$\left(\mathbf{I}_s \otimes \mathbf{V}^T\right)^{-1} = \mathbf{I}_s \otimes \mathbf{V},$$

to conclude that

$$\begin{aligned} \mathbf{x}_{k+1}^\delta = &\mathbf{x}_k^\delta + \left(\mathbf{b}^T \otimes \mathbf{V}\right)\left(\mathbf{A} \otimes \left[\operatorname{diag}\left(\sigma_i^2\right)_{n\times n}\right] + \alpha_k \mathsf{I}\right)^{-1} \\ &\times \left(\mathbf{I}_s \otimes \left[\operatorname{diag}\left(\sigma_i^2\right)_{n\times n}\right]\right)\left(\mathbf{1}_s \otimes \begin{bmatrix} \frac{1}{\sigma_1}\mathbf{u}_1^T \mathbf{r}_k^\delta \\ \vdots \\ \frac{1}{\sigma_n}\mathbf{u}_n^T \mathbf{r}_k^\delta \end{bmatrix}\right). \end{aligned} \tag{7.45}$$

The iterate (7.45) can be expressed as in (7.43) by taking into account that $\mathbf{X} = 1 \otimes \mathbf{X}$ and $\mathbf{x} = 1 \otimes \mathbf{x}$. The result is

$$\mathbf{F}_k = \left(\mathbf{b}^T \otimes \mathbf{I}_n\right)\left(\mathbf{A} \otimes \left[\operatorname{diag}\left(\sigma_i^2\right)_{n\times n}\right] + \alpha_k \mathsf{I}\right)^{-1}\left(\mathbf{1}_s \otimes \left[\operatorname{diag}\left(\sigma_i^2\right)_{n\times n}\right]\right).$$

Two extreme situations can be considered. If α_k is very small, then by virtue of the identity $\mathbf{b}^T\mathbf{A}^{-1}\mathbf{1}_s = 1$, which holds true for the Radau and Lobatto methods illustrated in Figure 7.13, we obtain $\mathbf{F}_k \approx \mathbf{I}_n$. On the other hand, if α_k is very large, the consistency relation $\mathbf{b}^T\mathbf{1}_s = 1$, yields $\mathbf{F}_k \approx (1/\alpha_k)\left[\operatorname{diag}\left(\sigma_i^2\right)_{n\times n}\right]$. Thus, the filter matrix of the Runge–Kutta regularization method behaves like the 'Tikhonov filter matrix'.

The exponential Euler method is based on the variation-of-constants formula which allows us to integrate the linear part of semilinear differential equations exactly. For the Showalter differential equation (7.29), Hochbruck et al. (2009) proposed the following modification of the original exponential Euler scheme:

$$\mathbf{x}_{k+1}^\delta = \mathbf{x}_k^\delta + \tau_k \varphi\left(-\tau_k \mathbf{K}_k^T \mathbf{K}_k\right)\mathbf{K}_k^T \mathbf{r}_k^\delta, \quad k = 0, 1, \ldots,$$

with

$$\varphi(z) = \frac{\mathrm{e}^z - 1}{z}.$$

Assuming the singular value decomposition $\mathbf{K}_k = \mathbf{U}\Sigma\mathbf{V}^T$ and setting $\alpha_k = 1/\tau_k$, the matrix function can be expressed as

$$\varphi\left(-\alpha_k^{-1}\mathbf{K}_k^T\mathbf{K}_k\right) = \alpha_k \mathbf{V}\left[\operatorname{diag}\left(\frac{1 - \exp\left(-\frac{\sigma_i^2}{\alpha_k}\right)}{\sigma_i^2}\right)_{n\times n}\right]\mathbf{V}^T, \tag{7.46}$$

and the iteration takes the form

$$\mathbf{x}_{k+1}^{\delta} = \mathbf{x}_k^{\delta} + \sum_{i=1}^{n} \left[1 - \exp\left(-\frac{\sigma_i^2}{\alpha_k}\right)\right] \frac{1}{\sigma_i} \left(\mathbf{u}_i^T \mathbf{r}_k^{\delta}\right) \mathbf{v}_i, \quad k = 0, 1, \ldots. \tag{7.47}$$

The exponential Euler regularization method is very similar to the regularizing Levenberg–Marquardt method in which the Tikhonov filter factors (7.44) are replaced by the filter factors

$$f_k\left(\sigma_i^2\right) = 1 - \exp\left(-\frac{\sigma_i^2}{\alpha_k}\right).$$

Obviously, the filter factors for the exponential Euler regularization method are close to 1 for large σ_i and much smaller than 1 for small σ_i.

The algorithmic implementation of asymptotic regularization methods resembles that of the regularizing Levenberg–Marquardt method. The main features are as follows:

(1) the iterations (7.41) and (7.47) are applied to the standard-form problem;
(2) the regularization parameters are chosen as the terms of a decreasing sequence $\alpha_k = q_k \alpha_{k-1}$ with constant or variable ratio q_k;
(3) a step-length procedure for the nonlinear residual is used to improve the stability of the method.

Note that the step-length procedure can be used because the Newton step $\mathbf{p}_k^{\delta}$ can be expressed as $\mathbf{p}_k^{\delta} = \hat{\mathbf{G}}_k \mathbf{K}_k^T \mathbf{r}_k^{\delta}$, where $\hat{\mathbf{G}}_k$ is a positive definite matrix; for example, in the exponential Euler regularization method, we have $\hat{\mathbf{G}}_k = \alpha_k^{-1} \varphi\left(-\alpha_k^{-1} \mathbf{K}_k^T \mathbf{K}_k\right)$, with $\varphi\left(-\alpha_k^{-1} \mathbf{K}_k^T \mathbf{K}_k\right)$ being given by (7.46).

The numerical performance of asymptotic regularization methods and of the regularizing Levenberg–Marquardt are comparable; for large initial values of the regularization parameters, the solution errors as well as the number of iteration steps are similar (Figure 7.14).

The asymptotic regularization methods yield results of comparable accuracies, although the solution errors given in Table 7.3 indicate a slight superiority of the Radau regularization method, especially for the O_3 retrieval test problem.

7.4 Mathematical results and further reading

The convergence of the nonlinear Landweber iteration is expressed by the following result (Hanke et al., 1995): if $x^{\dagger}$ is a solution of the equation $F(x) = y$ in the ball $B_{\rho}(x_{\mathtt{a}})$ of radius ρ about $x_{\mathtt{a}}$, F has the local property

$$\|F(x) - F(x') - F'(x')(x - x')\| \leq \eta \|F(x) - F(x')\|, \quad 0 < \eta < \frac{1}{2}, \tag{7.48}$$

for all $x, x' \in \mathcal{B}_{2\rho}(x_{\mathtt{a}})$, and the equation $F(x) = y$ is properly scaled in the sense that

$$\|F'(x)\| \leq 1, \quad x \in \mathcal{B}_{2\rho}(x_{\mathtt{a}}),$$

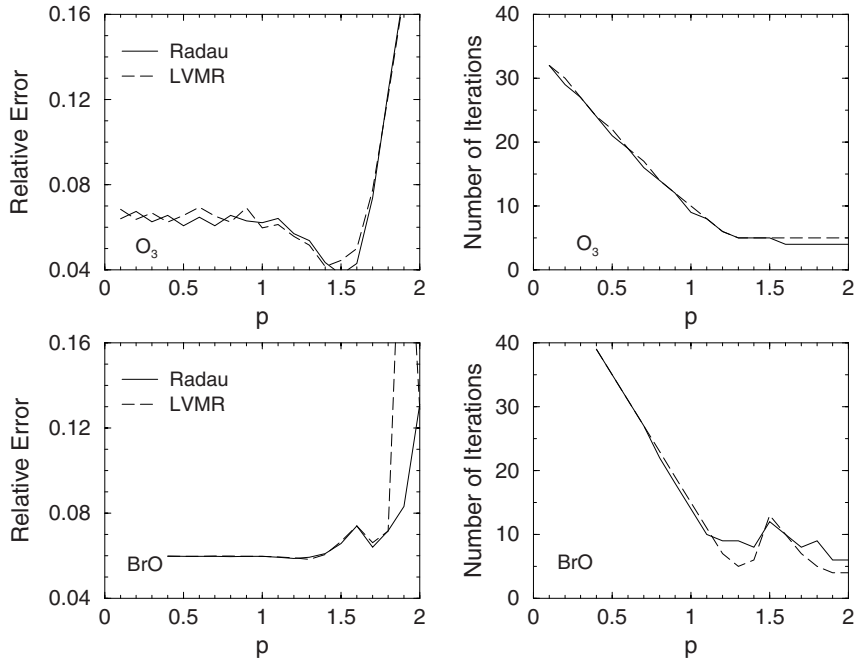

Fig. 7.14. Relative solution errors and the number of iteration steps for the Radau regularization method and the regularizing Levenberg–Marquardt (LVMR) method.

Table 7.3. Relative solution errors for Radau, Lobatto and exponential Euler regularization methods. The initial value of the regularization parameter is $\alpha = \sigma^p$.

			Selection criterion		
Problem	Method	p	S1	S2	S3
O_3	Radau	1.5	3.78e-2	3.78e-2	4.11e-2
	Lobatto		4.19e-2	4.19e-2	4.73e-2
	Euler		4.08e-2	4.08e-2	4.51e-2
BrO	Radau	1.2	5.88e-2	7.01e-2	5.82e-2
	Lobatto		5.87e-2	6.89e-2	6.92e-2
	Euler		5.88e-2	6.91e-2	6.09e-2
CO	Radau	1.0	3.72e-2	31.9e-2	3.75e-2
	Lobatto		3.79e-2	31.5e-2	3.59e-2
	Euler		3.78e-2	34.4e-2	3.27e-2
Temperature	Radau	0.9	1.80e-2	2.07e-2	2.06e-2
	Lobatto		1.80e-2	2.13e-2	2.10e-2
	Euler		1.80e-2	2.17e-2	2.07e-2

then $x_{k^\star}^\delta \to x^\dagger$ as $\Delta \to 0$, where $k^\star = k^\star(\Delta)$ is the stopping index of the discrepancy principle

$$\left\|y^\delta - F\left(x_{k^\star}^\delta\right)\right\| \le \tau_{\mathtt{dp}}\Delta < \left\|y^\delta - F\left(x_k^\delta\right)\right\|, \quad 0 \le k < k^\star,$$

and

$$\tau_{\mathtt{dp}} > 2\frac{1+\eta}{1-2\eta} > 2.$$

In contrast to Tikhonov regularization, the source condition

$$x^\dagger - x_{\mathtt{a}} = \left[F'\left(x^\dagger\right)^\star F'\left(x^\dagger\right)\right]^\mu z, \tag{7.49}$$

with $\mu > 0$ and $z \in X$, is not sufficient to obtain convergence rates. In Hanke et al. (1995), the convergence rate $O(\Delta^{2\mu/(2\mu+1)})$ with $0 < \mu \le 1/2$, has been proven under the additional assumption that, for all $x \in \mathcal{B}_{2\rho}(x_{\mathtt{a}})$, F satisfies

$$\begin{aligned} F'(x) &= R_x F'\left(x^\dagger\right), \\ \|I - R_x\| &\le c_{\mathtt{R}}\left\|x - x^\dagger\right\|, \quad c_{\mathtt{R}} > 0, \end{aligned} \tag{7.50}$$

where $\{R_x / x \in \mathcal{B}_{2\rho}(x_{\mathtt{a}})\}$ is a family of bounded linear operators $R_x : Y \to Y$.

The iteratively regularized Gauss–Newton method was introduced by Bakushinsky. In Bakushinsky (1992) local convergence was proven under the source condition (7.49) with $\mu \ge 1$, provided that F' is Lipschitz continuous, i.e.,

$$\left\|F'(x) - F'(x')\right\| \le L\|x - x'\|, \quad L > 0,$$

for all $x, x' \in \mathcal{B}_{2\rho}(x_{\mathtt{a}})$. Lipschitz continuity of F' suffices to prove convergence rates for the case $\mu \ge 1/2$, but if $\mu < 1/2$ further conditions, that guarantee that the linearization is not too far away from the nonlinear operator, are required. In Blaschke et al. (1997), the convergence rates

$$\left\|x_{k^\star}^\delta - x^\dagger\right\| = \begin{cases} o\left(\Delta^{\frac{2\mu}{2\mu+1}}\right), & 0 < \mu < 1/2, \\ O\left(\sqrt{\Delta}\right), & \mu = 1/2, \end{cases} \tag{7.51}$$

with $k^\star = k^\star(\Delta)$ being the stopping index of the discrepancy principle, have been derived by assuming the following restrictions on the nonlinearity of F:

$$\begin{aligned} F'(x) &= R(x, x')F'(x') + Q(x, x'), \\ \|I - R(x, x')\| &\le c_{\mathtt{R}}, \\ \|Q(x, x')\| &\le c_{\mathtt{Q}}\left\|F'\left(x^\dagger\right)(x - x')\right\|, \quad c_{\mathtt{R}}, c_{\mathtt{Q}} > 0, \end{aligned} \tag{7.52}$$

for all $x, x' \in \mathcal{B}_{2\rho}(x_{\mathtt{a}})$. Similarly, the optimal error bound $O(\Delta^{2\mu/(2\mu+1)})$ for $0 < \mu < 1/2$ has been proven by Bauer and Hohage (2005) for the Lepskij stopping rule and the nonlinearity assumptions (7.52). As the best convergence rate of the discrepancy principle is $O(\sqrt{\Delta})$, the generalized discrepancy principle

$$\alpha_{k^\star}\left\langle y^\delta - F\left(x_{k^\star}^\delta\right), \left[F'\left(x_{k^\star}^\delta\right)F'\left(x_{k^\star}^\delta\right)^\star + \alpha_{k^\star} I\right]^{-1}\left[y^\delta - F\left(x_{k^\star}^\delta\right)\right]\right\rangle \le \tau\Delta^2, \quad \tau > 1,$$

has been considered in Jin (2000), where the optimal convergence rate $O(\Delta^{2\mu/(2\mu+1)})$ with $0 < \mu \leq 1$ has been established under the nonlinearity assumptions:

$$[F'(x) - F'(x')]\, z = F'(x')\, h(x, x', z),$$
$$\|h(x, x', z)\| \leq c_{\mathtt{R}} \|x - x'\| \|z\|, \;\; c_{\mathtt{R}} > 0,$$

for all $x, x' \in \mathcal{B}_\rho\left(x^\dagger\right)$.

Results on convergence rates under logarithmic source conditions can be found in Hohage (1997) for the iteratively regularized Gauss–Newton method, and in Deuflhard et al. (1998) for the nonlinear Landweber iteration.

For a general regularization method of the form

$$x_{k+1}^\delta = x_{\mathtt{a}} + g_{\alpha_k}\left(F'\left(x_k^\delta\right)^\star F'\left(x_k^\delta\right)\right) F'\left(x_k^\delta\right)^\star \left[y^\delta - F\left(x_k^\delta\right) + F'\left(x_k^\delta\right)\left(x_k^\delta - x_{\mathtt{a}}\right)\right], \tag{7.53}$$

the convergence rates (7.51) have been derived by Kaltenbacher (1997, 1998) for the modified discrepancy principle

$$\max\left(\left\|y^\delta - F\left(x_{k^\star-1}^\delta\right)\right\|, r_{\mathtt{1}k^\star}\right) \leq \tau_{\mathtt{dp}}\Delta < \max\left(\left\|y^\delta - F\left(x_{k-1}^\delta\right)\right\|, r_{\mathtt{1}k}\right), \;\; 1 \leq k < k^\star, \tag{7.54}$$

with

$$r_{\mathtt{1}k} = y^\delta - F\left(x_{k-1}^\delta\right) - F'\left(x_{k-1}^\delta\right)\left(x_k^\delta - x_{k-1}^\delta\right),$$

provided that $\tau_{\mathtt{dp}} > 1$ is sufficiently large, the nonlinearity conditions (7.52) hold, and the sequence $\{\alpha_k\}$ satisfies (7.7). Note that the stopping rule (7.54) is essentially equivalent to the termination criterion

$$\max\left(\left\|y^\delta - F\left(x_{k^\star-1}^\delta\right)\right\|, \left\|y^\delta - F\left(x_{k^\star}^\delta\right)\right\|\right)$$
$$\leq \tau'_{\mathtt{dp}}\Delta < \max\left(\left\|y^\delta - F\left(x_{k-1}^\delta\right)\right\|, \left\|y^\delta - F\left(x_k^\delta\right)\right\|\right), \;\; 1 \leq k < k^\star,$$

which stops the iteration as soon as the residual norms at two subsequent iteration steps are below $\tau'_{\mathtt{dp}}\Delta$. Examples of iterative methods having the form (7.53) are the iteratively regularized Gauss–Newton method with

$$g_\alpha(\lambda) = \frac{1}{\lambda + \alpha}$$

and the Newton–Landweber iteration with

$$g_\alpha(\lambda) = \frac{1}{\lambda}\left[1 - (1-\lambda)^p\right], \;\; \alpha = \frac{1}{p}.$$

Hanke (1997) established the convergence of the regularizing Levenberg–Marquardt method by using the local nonlinearity assumption

$$\|F(x) - F(x') - F'(x')(x - x')\| \leq c\|x - x'\| \|F(x) - F(x')\|, \;\; c > 0,$$

for all $x, x' \in \mathcal{B}_{2\rho}(x_{\mathtt{a}})$, and by choosing the regularization parameter α_k as the solution of the 'discrepancy principle' equation (cf. (7.19))

$$\left\|y^\delta - F\left(x_k^\delta\right) - F'\left(x_k^\delta\right)\left[x_{k+1}^\delta(\alpha) - x_k^\delta\right]\right\| = \theta\left\|y^\delta - F\left(x_k^\delta\right)\right\|,$$

for some $\theta \in (0, 1)$.

The regularizing trust-region method was analyzed by Wang and Yuan (2005). Convergence results have been proven under the nonlinearity assumption (7.48) with $0 < \eta < 1$, provided that the iterative process is stopped according to the discrepancy principle with

$$\tau_{\mathtt{dp}} > \frac{1+\eta}{1-\eta}.$$

Convergence rates for the regularized inexact Newton iteration method

$$x_{k+1}^{\delta} = x_k^{\delta} + g_{\alpha_k}\left(F'\left(x_k^{\delta}\right)^{\star} F'\left(x_k^{\delta}\right)\right) F'\left(x_k^{\delta}\right)^{\star}\left[y^{\delta} - F\left(x_k^{\delta}\right)\right], \tag{7.55}$$

and the source condition (7.49), have been established by Rieder (1999, 2003). The general iteration method (7.55) includes the regularizing Levenberg–Marquardt method, and Newton-type methods using as inner iteration the CGNR method, the Landweber iteration and the ν-method.

The convergence of the Runge–Kutta regularization method has been proven by Böckmann and Pornsawad (2008) under the nonlinearity assumption (7.48).

The recent monograph by Kaltenbacher et al. (2008) provides an exhaustive and pertinent analysis of iterative regularization methods for nonlinear ill-posed problems. In addition to the methods discussed in this chapter, convergence and convergence rate results can be found for the modified Landweber methods (iteratively regularized Landweber iteration, Landweber–Kaczmarz method), Broyden's method, multilevel methods and level set methods.

In Appendix H we derive convergence rate results for the general regularization methods (7.53) and (7.55) in a discrete setting. The regularization scheme (7.53) corresponds to the so-called Newton-type methods with a priori information, e.g., the iteratively regularized Gauss–Newton method, while the regularization scheme (7.55) corresponds to the Newton-type methods without a priori information, e.g., the regularizing Levenberg–Marquardt method.